1-1-2009

Description Of Associative Behaviour During Microbial Cellulose Utilization By Clostridium Thermocellum For Application In Advanced Biomass Conversion Process Development

Alexandru, Dumitrache
Ryerson University

DESCRIPTION OF ASSOCIATIVE BEHAVIOUR DURING MICROBIAL CELLULOSE UTILIZATION BY *CLOSTRIDIUM THERMOCELLUM* FOR APPLICATION IN ADVANCED BIOMASS CONVERSION PROCESS DEVELOPMENT

by

Alexandru Dumitrache, BSc. Applied Chemistry and Biology

Ryerson University, Toronto, Canada, 2006

A thesis

presented to Ryerson University

In partial fulfillment of the

requirements for the degree of

Master

In the Program of

Molecular Science

Toronto, Ontario, Canada, 2008

© Alexandru Dumitrache 2008

I hereby declare that I am the sole author of this thesis.

I authorize Ryerson University to lend this thesis to other institutions or individuals for the purpose of scholarly research.

I further authorize Ryerson University to reproduce this thesis by photocopying or by other means, in total or in part, at the request of other institutions or individuals for the purpose of scholarly research.

DESCRIPTION OF ASSOCIATIVE BEHAVIOUR DURING MICROBIAL CELLULOSE
UTILIZATION BY *CLOSTRIDIUM THERMOCELLUM* FOR APPLICATION IN ADVANCED
BIOMASS CONVERSION PROCESS DEVELOPMENT

Master of Science, 2009

Alexandru Dumitrache

Molecular Science, Ryerson University

ABSTRACT

Recent findings support the concept that *Clostridium thermocellum* is a cellulose-utilizing specialist having growth benefits with increasing substrate chain length. We developed a continuous-flow system for *in-situ* detection of cellulose colonization and qualitatively assayed metabolic activities and behavior of cellulolytic cultures. This study demonstrates the existence of strongly adherent cellulolytic cells arranged in monolayers with invariably end-on attached spores. The substrate-cell distance was recorded to be lower than 0.44μm and a typical EPS matrix was absent. Measurements on carbon dioxide released in continuous-flow cultures was successfully employed to monitor biofilm activity and total carbohydrate assays do not reveal loss of cellulolysis end-products in the effluent. These findings demonstrate the bacteria have optimized access to the cellulosic substrates and suggest that they have an ability to sequester products of substrate hydrolysis which confers benefits over non-adherent cellulolytic or non-cellulolytic organisms.

ACKNOWLEDGMENTS

TABLE OF CONTENTS

LIST OF TABLES

LIST OF FIGURES

INTRODUCTION

Thesis synopsis

In today's awakened consciousness for the need of a greener economy, plant biomass is considered a sustainable source for liquid fuels and biomaterials. Production of biofuels from grains is not sustainable; however cellulosic material is a cost-attractive and relatively abundant source of biofuel feedstock. A considerable impediment preventing the widespread utilization of lignocellulosic substrates is the inherent recalcitrance of the cellulosic biomass. A cost-reducing strategy, defined as "consolidated bioprocessing" (Lynd, 1996), has been proposed where the production of cellulolytic enzymes, the hydrolysis of biomass and the fermentation of resulting sugars to desired products occur in a single step process via the actions of a cellulolytic microorganism or consortium. Isolating and critically assessing organisms that posses the combined desired functions of substrate utilization and product formation are important steps towards advancing such strategies. To achieve this, an integrative approach where cellulose utilization is viewed from a microbial perspective as opposed to an enzymatic phenomenon, is desirable for future research advances that could be translated into technological progress (Lynd *et al*, 2002). The objective of this research was therefore to combine the well established fields of cellulose conversion and biofilm research to describe the association between anaerobic cellulolytic bacteria and their cellulosic substrates. Experimental continuous-flow systems were designed to enable simultaneous, real-time (confocal laser scanning microscopy, CLSM) analysis of cell

adherence to the cellulosic substrate and metabolic activity under fully hydrated, anaerobic conditions. Special modifications were made to facilitate measurements in cases where analytic procedures were not compatible with an anaerobic chamber. Cellulose fibers were immobilized in continuous-flow mini-reactors to serve as carbon source as well as attachment substratum, and inoculated with *Clostridium thermocellum* ATCC 27405 previously grown in batch. A peristaltic pump continuously fed the mini-reactors at a constant flow rate with RM medium (Ozkan *et al*, 2001) lacking a cellulosic carbon source (however, supplemented with 2g/L yeast extract). Flow cell volumes varied between 4mL and 10mL with residence times of thirty minutes to one hour. A novel approach was developed to measure whole population metabolic activity in real time based on carbon dioxide production rates. In essence, this method involves coupling of reactor effluent with a CO_2 exchange system linked to a carbon dioxide analyzer. Concomitantly, flow cell effluents were collected and assayed for total carbohydrate content, by the phenol-sulfuric acid protocol, and for total non-attached cell counts eluted from the flow chamber, by an adapted direct epifluorescence counting technique. An image analysis routine, based on the Zeiss LSM 510 and Daime imaging software (Daims *et al*, 2006), was developed to perform high resolution three-dimensional volume rendering of CSLM images.

Hypothesis

The central hypothesis of this research is that anaerobic gram positive *Clostridium thermocellum* bacteria strongly adhere to their cellulosic carbon substrates developing characteristic architectures that work towards optimizing the net energy gain from the utilization of cellulose. The attachment and proliferation around the sole

2

cellulosic carbon source provides an advantage for the optimal capture of the products released by cellulose hydrolysis with an implied minimal loss to the bulk aqueous phase.

Objectives

The overall goal was (i) to combine the field of biofilm research with the previous findings on cellulose utilization by anaerobic thermophilic cellulolytic bacteria and (ii) to address the question of the degree of microbe-substrate interaction. The predominantly common fermentation reactor studies have not expanded to carry *in-situ* observations on the associative behavior of these cellulolytic organisms; (iii) therefore our objective was to develop a continuous-flow mini-reactor system for the growth of thermophilic and strictly anaerobic bacteria and (iv) to perform high resolution imaging on the fully hydrated and undisturbed cultures. Additionally, assays performed on the effluent feed of these mini-reactors were used (v) to qualitative asses the degree of culture activity and microbial behavior during growth in the presence of immobilized solid cellulosic material as the sole carbon source.

CHAPTER 1. LITERATURE REVIEW

1.1. Energy biotechnology and microbial conversion of biomass through consolidated bioprocessing (CBP)

The emergent field of energy biotechnology is concerned with alternative research areas for the conversion of biologically derived solar energy through either biological or non-biological process steps (e.g. product recovery) (Lynd, 2008). Important biological energy conversion processes (Figure 1.1) are: biocatalytic systems, which use reduced electron carriers derived from water that can be subsequently oxidized to produce electricity or hydrogen; aquatic biomass in the form of cyanobacteria, algae and diatoms (or aquatic microbial oxygenic photoautotrophs - AMOPs) that can be mass produced with high yields to serve as synthetic fuel precursors (such as oil and fatty acids) (Dismukes *et al*, 2008); terrestrial biomass conversion to fuels with strategies diverging into three main efforts: feedstock production, biomass recalcitrance and product formation (Lynd, 2008).

Feedstock production originates from recovered waste materials (Wyman and Goodman, 1993; Lynd, 1996) or from the conversion of sunlight to plant biomass with an emphasis on high land productivity with feasible economic impacts and a low ecological footprint. Using biomass to produce biofuels on large scale is foreseen as a more sustainable and secure option that it was in the past by focusing on the cost-

effective potential of bioenergy technologies when they are commercially mature, and by integrating agricultural products with growing biomass (Greene *et al*, 2004).
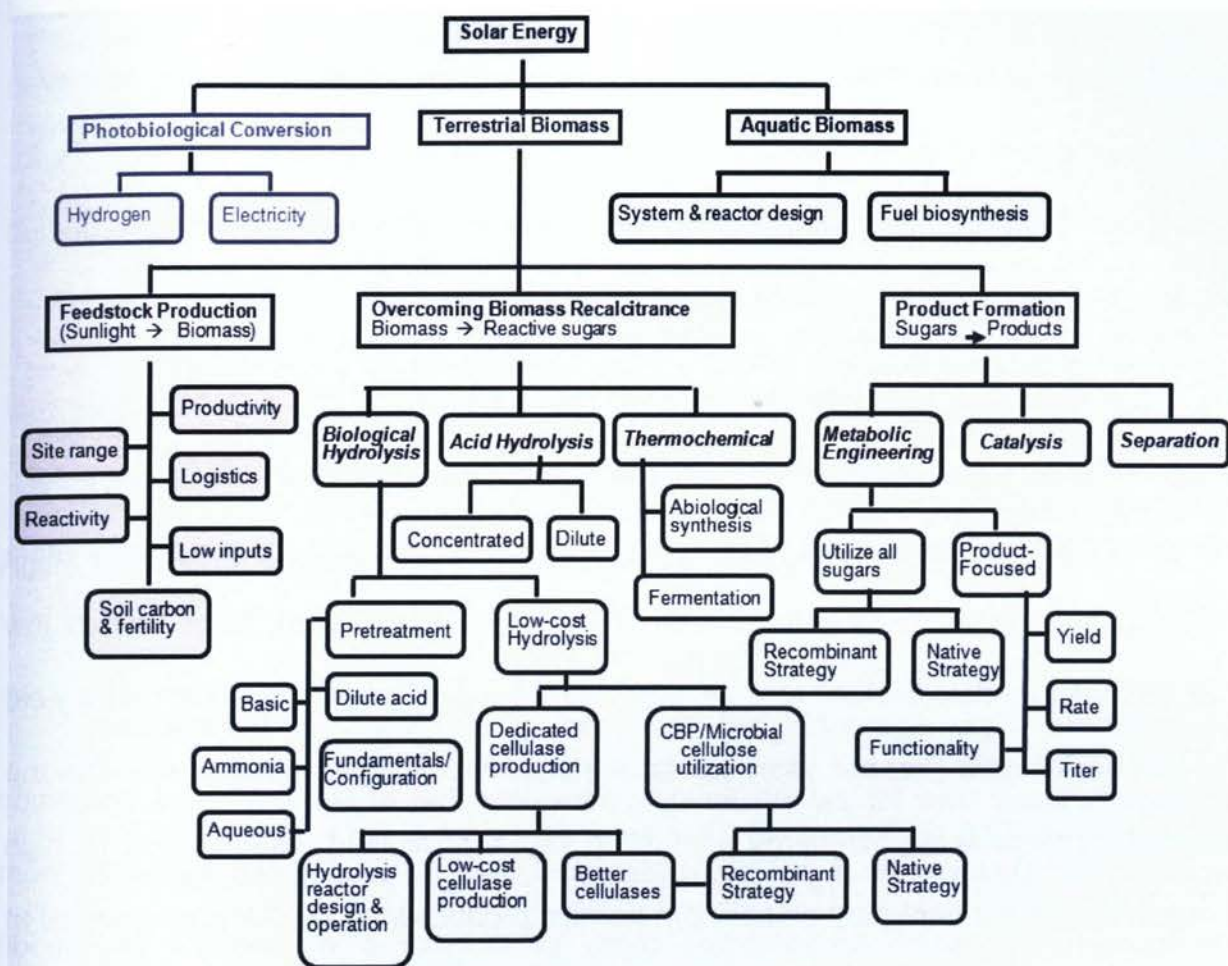
Figure 1.1 Biological energy conversion processes. Adopted from Lynd, L.R., 2008.

New metrics that correctly estimate resource inputs and environmental factors need further development. Nevertheless, recent studies indicate that lignocellulosic biomass can achieve energy production (primarily ethanol at the center of most research data) with a decisively positive balance for energy return on investment (Farrell *et al*, 2006; Hammerschlag, 2006; Wyman, 2008).

Agricultural multifunctional systems, defined as the joint production of commodities such as food and fiber together with ecological services such as cellulosic crop production are recognized to have environmental benefits which include: reduced soil and nitrogen loss rates, increased greenhouse gas sequestration and improved water quality and wildlife habitat. Perennial plant species are seen as the basis for biomass production on agricultural systems with mixed multiple species, three cropping farmlands and managed wetlands (Jordan *et al*, 2007).

Cellulosic material such as perennial grass (e.g. switch grass) is especially well suited for large scale energy production due to their low production cost (Figure 1.2). Estimates place cellulosic crops at $50/metric ton or converted to price per energy value at $3/GJ, which is comparable to oil at $17/barrel (Lynd *et al*, 2008). Aside from its low cost, biomass feedstock must also be available on a very large scale. Land fuel yield (GJ fuel per hectare (ha) per year) values are important critical figures in securing the potential for large scale bioenergy production with a finite land resource and its high competitive use. Current data places corn kernels production at 85 GJ/ha and soy oil at 18 GJ/ha but land fuel yield estimates on cellulosic biomass score much higher at 135 GJ/ha with the potential to substantially increase with future development in crops and cropping systems (Lynd *et al*, 2008).

Although feedstock production is foreseen to eventually become the dominant industry determinant or the indicator of the extent to which the industry can expand in the future, a primary current identifiable bottleneck remains the initial conversion of biomass to sugars dominated by the difficulty in processing, or the recalcitrance, of lignocellulosic material (Lynd, 2008).

Energy source	Price	
	Common ($/amount)	$/GJ[a]
Petroleum	50/bbl	8.7
Gasoline[b]	1.67/gallon	13.7
Natural gas[c]	7.50/scf	7.9
Coal[d]	20/ton	0.9
Coal with carbon capture[e,f]	106/ton	4.8
Electricity	0.04/kWh	11.1
Soy oil[g]	0.23/lb	13.8
Corn kernels[h]	2.30/bu	6.6
Cellulosic crops[i]	50/ton	3.0

[a]Assumed lower heating values: petroleum, 5.8 GJ/bbl; gasoline, 5.1 GJ/bbl; natural gas, 37.3 MJ/m^3; coal, 23.3 MJ/kg; soy oil, 36.8 MJ/kg; corn kernels, 16.3 MJ/kg; cellulosic crops, 17.4 MJ/kg. [b]Wholesale price, average 2004–2006 (ref. 21). [c]2005 annual average US wellhead price[21]. [d]2004 annual average US open market price[21]. [e]Cost of carbon capture assumed to be $150/ton carbon[22]. [f]Coal carbon content assumed to be 57% (dry weight basis)[23]. [g]Average price 2004–2005 (ref. 19). [h]Average price 2002–2005 (ref. 24). [i]Price representative of typical values assumed for energy crops in the literature (for example, McLaughlin et al.[25]). bbl, barrel; scf, standard cubic foot.

Figure 1.2 Values of potential energy sources. Adopted from Lynd et al, 2008

Independent on variations in structure, the plant cell wall contains most commonly between 35% to 50% cellulose of plant dry weight and is considered the most abundant component of plant biomass. However, in most cases the cellulose fibers are encased in a network of other biopolymers, primarily hemicelluloses representing between 20% to 35% of the plant dry weight and lignin in the range of 5% to 30% (Lynd et al, 2002). It is this typical structural feature of cell wall matrix that limits the rate and extent of utilization of whole, untreated plant biomass. Recalcitrance reduction strategies are currently seen as thermochemical processes with production of low molecular weight gases and liquids (gasification and pyrolysis, respectively); dilute or concentrated acid hydrolysis which is known to produce low and high sugar yields respectively, with the condition that the latter requires acid recovery process steps to render it cost-efficient; and biological hydrolysis using cells or enzymes (Lynd, 2008).

The biological approach has the beneficial property that it can utilize a large spectrum of biomass but it requires pre-treatment to make the cellulose readily available to hydrolytic attack. Fermentation studies on naturally occurring plant material, incubated in the presence of pure culture cellulolytic organisms or cell-free enzyme (cellulase) preparations have shown cellulose hydrolysis yields that are under 20% of the theoretical expectations, therefore feedstock pretreatment is seen as a defining step in biomass conversion processes (Lynd et al, 2002). Biologically mediated conversion processes feature the following general steps: enzyme production, cellulose hydrolysis (and hydrolysis of other insoluble polysaccharides), and fermentation of cellulose and hemicellulose hydrolysis products. Most process developments to date have in common the dedicated initial step of cellulase production (Figure 1.3) (Lynd et al, 2002); however, a configuration where the four transformations occur in a single step, called consolidated bioprocessing (CBP), has been proposed and estimated to have great potential for cost-reducing efforts.

The total cost of advanced CBP was rounded to approximately 23% of the simultaneous saccharification and co-fermentation strategy (Figure 1.4) (Lynd et al, 2005), and although cellulase production costs followed a greater than tenfold reduction and have been recently estimated to 30cents/gallon ethanol (Lynd et al, 2008) that does not diminish the potential of consolidated bioprocessing for achieving low cost hydrolysis.
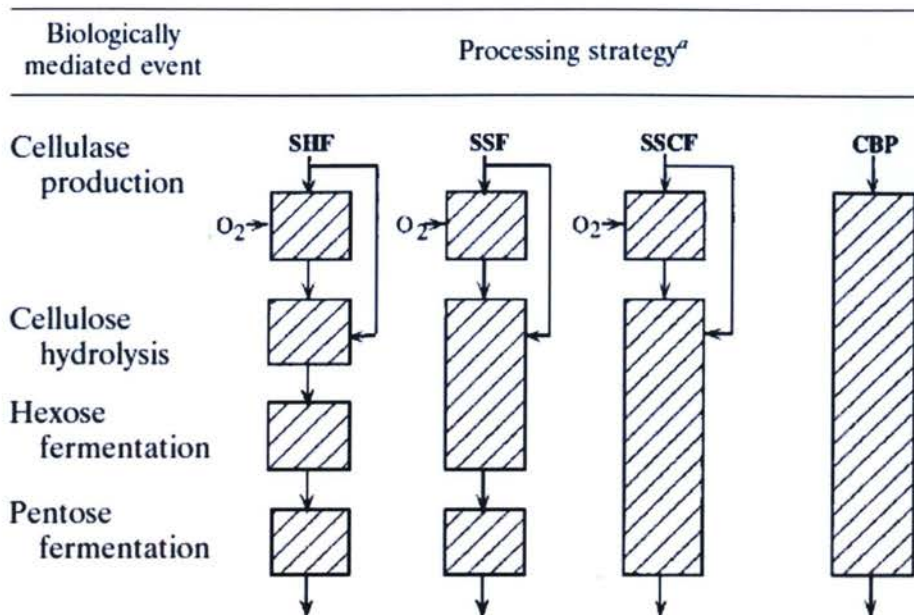
Figure 1.3 Evolution of biomass-processing schemes featuring enzymatic hydrolisys and single-step consolidated bioprocessing. Adopted from Lynd *et al*, 2002.

(SHF)Separate hydrolysis and fermentation; (SSF) Simultaneous saccharification and fermentation; (SSCF) Simultaneous saccharification and co-fermentation
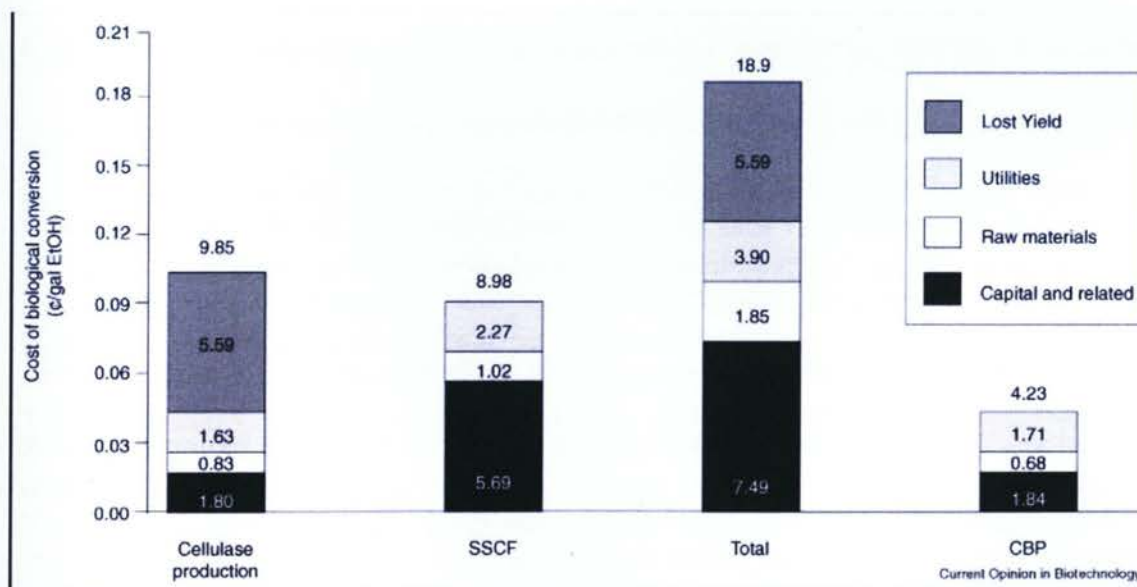
Figure 1.4 The comparative cost of ethanol production by consolidated bioprocessing (CBP) and by simultaneous saccharification and co-fermentation (SSCF) featuring dedicated cellulase production. Adopted from Lynd *et al*, 2005.

9

In CBP configuration, where the conversion is seen from a microbial perspective rather than an enzymatic reaction, lower costs are derived from reduced reactor volume and capital investments and higher hydrolysis rates due in part to enzyme-microbe synergies and cellulose adherent cellulolytic organisms that are likely to compete for products of hydrolysis with the non-attached organisms (including reactor contaminants) (Lynd *et al*, 2005). Organism development approaches for consolidated bioprocessing can be classified as native cellulolytic strategies for improvements of product formation properties of organisms that already utilize the substrate well, e.g. *Clostridium thermocellum* (Tyurin *et al*, 2004) and *Thermoanaerbacterium saccharolyticum* (Mai and Wiegel, 2000); or recombinant cellulolytic strategies for improvements of substrate utilization properties of organisms that already have strong product formation potential, e.g. *Saccharomyces cerevisiae* (Van Zyl *et al*, 2007). To date, no organism that meets both requirements is known. *Clostridium thermocellum*, the subject of study in this research, is a starting point candidate for CBP development, being a native cellulolytic, cellulosome producing microbe, but unable to ferment pentoses.

The future of research and development is believed to offer much larger cost-savings from improvements in converting biomass to sugars in comparison to the conversion of sugars to fuels (Lynd *et al*, 2008). However, about the latter process it is worth mentioning that the diversification of fuel molecules can be expected to expand once the cellulosic biofuels technology becomes established. Also metabolic engineering of microorganisms, directed towards the production of commercially desirable goods (e.g. 1, 2 propane diol, lactic acid) as chemical coproducts for smaller markets are a beneficial economic incentive.

1.2. Microbial biofilms

1.2.1. Biofilms as a bacterial developmental process

Bacteria are often studied in a planktonic mode of life as suspended cells growing in a liquid environment, however, in most natural environments, association with a surface is the most prevailing microbial lifestyle, with some figures indicating an overwhelming 95%-99% of microorganisms existing in this mode, called "biofilm" (Nikolaev and Plakunov, 2007). The sessile bacteria thrive in multicellular communities associated with phase interfaces which convey those advantages over individual cells, most notably protection against environmental factors such as extreme conditions, host immune response, predation and antimicrobial stress. The classical biofilm is a microbial consortium of adherent cells, situated (most commonly) at a liquid solid interface and encased within a matrix of extracellular polymeric material. This definition also includes microbial aggregates and flocules (Costerton, 1995). Biofilm translocation to new niches is generally understood through the yield of cells from the sessile state back into the planktonic mode with subsequent recolonization of new interfaces, or in the case of some flagellated bacteria by a massive coordinated group behavior called swarming motility (Verstraeten *et al*, 2008). Other surface-associated methods of translocation have been described (Henrichsen, 1972). Taken to the extreme, the planktonic mode of bacterial life can therefore be viewed as primary mechanisms of cell translocation from one surface to another (Watnick and Kolter, 2000), however, from a holistic perspective both biofilm and planktonic phenotypes are seen as integrated

components of the prokaryotic lifestyle (Stoodley *et al*, 2002). Biofilms are also seen as developmental stages of bacterial life cycles with many studies suggesting that the profile of gene transcription is significantly distinct in the adherent cell form (Prigent-Combaret *et al*, 1999) and that cell to cell signaling is a required condition for structure formation (Davies *et al*, 1998; Purevdorj *et al*, 2002). It is generally accepted that biofilms follow, with large variations from species to species, a multiple step-by-step development. Stoodley *et al* described their formation as a five step process, starting with initial attachment of cells to an interface, the production of extracellular polymeric substances (EPS) to strengthen the nonspecific adhesion, early development of biofilm structures, maturation into larger architectures and cell dispersion from the biofilm matrix (Stoodley *et al*, 2002). However, it is acknowledged that cell detachment, a developmental closing stage which returns cells into the planktonic lifecycle, is still largely not understood, with relatively few studies having been conducted to elucidate the biological basis for this process. For example, in some cases cell detachment from substratum has been correlated with the very onset of the stationary cell phase. With regards to the initial process of biofilms formation, although a large variability is expected to exist, at least three distinct mechanisms have been proposed. First, an initial dispersed attachment of cells followed by aggregation in clusters mediated through surface motility, such as the case of type IV pili-mediated twitching motility of *Pseudomonas aeruginosa* (O'Toole and Kolter, 1998). A second mechanism is by binary division of adherent cells with subsequent sprawling outward and upward (in many cases) with the formation of complex multicellular architectures (Heydorn *et al*, 2000b). A third mechanism proposes microbial aggregation by continuous recruitment

12

of cells from the bulk liquid phase into the sessile mode (Tolker-Nielsen *et al*, 2000). However, the actual mechanism employed in any particular case might result from a combination of factors such as the organisms being involved, the nature of the attachment surface and the physical and chemical properties of the present environment (Stoodley *et al*, 2002).

1.2.2. **Biofilm investigation tools and studies on anaerobic microbial communities**

In the past decades much effort has been made to elucidate the mechanisms of cell adhesion and the structures and functions of biofilms in natural and engineered environments. The importance of biofilm research spans across multiple disciplines and efforts focus for the most part on either promoting or inhibiting biofilm processes. In broad general examples, understanding biofilm growth and potential ways to limit and monitor it are important in preventing biofouling of surfaces (Beech *et al*, 2005; Coetser and Cloete, 2005) and biofilm-induced conditions in humans and infections in implant surgeries (Hall-Stoodley and Stoodley, 2005; Nejadnik *et al*, 2008); conversely, improving biofilm performance have been sought for effective wasterwater treatment strategies (Krzanowski and Walega, 2008; Yun *et al*, 2006) or for promoting plant growth when used as biocontrol agents for example (Bais *et al*, 2004). As mentioned in the previous section, seeking strategies to improve biomass conversion with the use of

cellulose adherent microorganisms is another example of an engineered system where biofilm research has potential use.

Modern biofilm research has relied heavily on several major approaches: genetic screening on various deficient mutants (Kim *et al*, 2008; Kobayashi, 2008), the application of confocal laser scanning microscopy in conjunction with new fluorescent molecular probes and digital image analysis (Larsen *et al*, 2008; Merod *et al*, 2007), and to a lesser extent through biophysical studies that measure adhesion kinetics and cohesive strength (e.g. the quartz crystal microbalance technique, atomic force microscopy or the optical tweezers) (Otto, 2008). These do not, however, diminish the research potential for the application of virtually unlimited cross-disciplinary tools with examples such as measurements on biofilm respiratory activity (Simões *et al*, 2007), quantification of cell mass and numbers (Jensen *et al*, 2008) and biochemical, spectroscopic and chromatographic analysis of cells and EPS composition and structure (Rau *et al*, 2008).

In-situ observations of biofilm samples are usually made in real time under flow conditions with typically the use of flow cells (Palmer, 1999). The flow chamber allows the growth of microbial biofilms on solid surfaces under controlled conditions and their microscopic visualization through a transparent window under fully hydrated conditions and in a non-destructive manner, with the possibility of repeated observation over long cultivation periods and the extrapolation of behavioral changes.

The study of anaerobic biofilms has been much less common than the aerobic counterpart, and with relevance to this thesis, the research on cellulose degrading

communities, either in pure culture or consortia, is being evaluated. While past studies on microbial cellulose degradation are numerous, the principal approach to understanding organism behavior and cellulose colonization were made by collecting slurry samples from fermentation reactors and subjecting them to light and fluorescence microscopy, fluorescence in-situ hybridization and electron microscopy (O'Sullivan et al, 2005; Syutsubo et al, 2005; Bayer et al, 1998) or indirectly by molecular and biochemical probing of batch cultures (Gelhaye et al, 1992). Arguably, the former methods have a destructive nature associated with sample preparation and can skew their observation on the complexity of adherent structures and the latter methods do not provide insights on colonization properties or spatial relationships. Studies on cellulolytic biofilms using the non-destructive approach of flow cells are few and relatively recent. A study of the colonization potential of naturally occurring, mixed species in the anaerobic layers of a landfill site made use of an adapted aerobic flow cell to promote strict anaerobic conditions (Jones et al, 1997). The culture chamber, designated as the anaerobic continuous culture microscopy unit (ACCMU), was a miniature, self-sealing, oxygen impermeable, transparent reactor that could be fit on a microscope stage. The investigators used inoculums of enriched collections from the anaerobic layers of a landfill site, which were injected at the outflow port of the flow chamber to avoid passive transport of organisms by the media flow and to ensure that any observed attachment upstream was due to some active motility or transposition event. The colonization process on biodegradable and non-biodegradable materials was monitored over time by capturing phase contrast micrographs and calculating the rate of the "biofilm front" advance. Fluorescence microscopy and the natural F_{420} autofluorescence were used to

track and quantify the localization of methanogenic bacteria. It was found that wood, cotton and polyester fabric remained poorly colonized or not colonized after weeks of incubations, whereas the non-biodegradable glass, plastic and polyethane were readily and heavily colonized. However the study acknowledged that enrichement for butyrate and hexanoate degrading methanogens could have excluded cellulolytic organisms from the flow cell inoculums which could explain the lack of cellulose colonization.

A different study used the flow cell to grow pure cultures of the oral bacteria *Porphyromonas gingivalis* under anaerobic and micro-aerophilic conditions (Hansen *et al*, 2000). Their findings show poor biofilm formation after 18 hours of growth under low oxygen concentrations (1-2 ppm) and improved growth in anaerobic culturing. For anaerobic conditions, the system made use of an inflatable glove chamber to isolate the medium flask (kept under continuous $N:CO_2$ sparging) and the flow cell from the normal atmosphere environment. Biofilm formation was visualized with fluorescence tagging and confocal laser microscopy. An extensive literature review revealed that growth of anaerobic biofilms has been attempted only a few times and that the most commonly used anaerobic chemostat technology had not been extended to perform *in-situ* observations.

A recent article where microbial attachment and cellulose degradation in leachate and rumen systems was evaluated *in-situ* and in real time acknowledges the high potential and utility of using flow cell concepts in the study of anaerobic biofilms (O'Sullivan *et al*, 2008b). In their system, a flow cell, which contained immobilized cellulose fibers on the underside of the glass coverslips, was connected to an anaerobic flask media (containing crystalline cellulose) in a closed loop so that its content is

continuously re-circulated through the flow chamber. The media flask was inoculated with rumen fluid or anaerobic leachate from a municipal solid waste digester and during the incubation the extent of cellulose solubilisation was estimated by nitrogen/COD balance. Concurrently, phase contrast microscopy was used to estimate the extent of biofilm formation at the cellulose interface inside the flow cell. The study aimed to correlate the imaging of cellulolytic biofilm with process performance data in real time, and the results suggest that the rumen culture formed thicker and more stable biofilms than the inoculum from digester leachate, which were consistent with the faster rates of cellulose solubilisation in the rumen reactors. It is also acknowledged that the presence of multilayer biofilms could be partly due to the interactions between the species within the microbial consortia and that close interactions between bacteria and cellulose particles are required for efficient cellulose degradation.

1.3. Cell substrate interactions in microbial cellulose utilization

The close associations between cellulolytic organisms and their substrate have been reported in the literature since the early 1980's. For example, a survey of 13 cellulolytic and 10 non-cellulolytic strains of *Ruminococcus albus* showed that most cellulolytic strains bind to the substrate whereas most non-cellulolytic strains do not, however the bacterial adhesion was not well correlated to the cellulolytic activity of the cultures (Morris and Cole, 1987). A review on the biological degradation of cellulose

17

(Béguin and Aubert, 1994), where the primary focus was set on understanding the structure and activity of cellulolytic enzymes, acknowledges that microbe-substrate interactions are an obvious advantage towards optimizing the recovery of soluble hydrolysis products. The means of interactions were reported presumably through extracellular cellulases secreted by the microorganisms or by cellulose-binding components present on the cell surface.

In the case of *C. thermocellum*, cellulolytic enzyme complexes, defined as cellulosomes (see discussion on cellulosome below in Section 1.4) were found to form large clusters embedded in the cell surface layer, appearing as protuberances in electron micrographs. Mutants isolated from their inability to bind cellulose were found to lack such protuberances of cell-bound cellulosomes and to display reduced cellulose hydrolysis rates (Bayer *et al*, 1983; Bayer *et al*, 1985; Bayer and Lamed, 1986). Later advancements in molecular biology allowed the full description of the macromolecular cellulosome machineries where a non-cellulolytic scaffoldin module – the cellulose-binding domain (CBD) - was responsible for binding the cellulase complex to the substrate and in some cellulosomes, multiple-domain anchoring proteins were found to connect the enzyme complex to the cell surface (Bayer *et al*, 1998). Other investigations using electron microscopy revealed that such cell surface "protuberances" with similar morphology are present on the surface of a variety of cellulolytic bacteria (gram positive or negative, thermophilic or mesophilic, aerobic or anaerobic) but they are not found in non-cellulolytic bacteria or on cellulolytic bacteria grown in conditions that are known to repress cellulase synthesis (Lamed *et al*, 1987; Hostalka *et al*, 1992).

Rumen bacteria are known to present strong attachment to substrates. Electron micrographs of the cellulolytic rumen bacteria *Fibrobacter succinogenes* shows its tight adherence to the cellulose fibers with erosion present beneath the cells (Gaudet and Gaillard, 1987). Glycosylated residues of cellulose-binding proteins (CBP), some of which have endoglucanase activity, isolated from the cell envelope of *Fibrobacter intestinalis* DR7 were suggested to have an important role in the adhesion of cells to cellulose (Miron *et al*, 1999), and electron micrographs of adherent *Ruminococcus flavifaciens* cells have shown the presence of a discernable exopolysaccharide network, presumably responsible for non-specific adhesion (Kudo *et al*, 1987). A glycocalyx, responsible for substrate adherence through its constitutive polymeric elements, has also been identified in the anaerobic cellulolytic *Ruminococcus albus* 7. Variable-pressure scanning electron microscopy revealed the formation of thin cellular extensions that mediate substrate attachment, followed by the development of a ramifying network that connects individual cells to one another (Weimer *et al*, 2006). Additionally, in gram positive *R. albus* 8 strain a novel type of cellulose-binding protein (cbcC) belonging to the Pil-protein family has been isolated. Being most similar to the type 4 fimbrial proteins of gram-negative pathogenic bacteria, the anaerobe was indicated to produce a fimbriae mechanism in its adhesion to cellulose (Morrison and Miron, 2000).

To summarize, the adhesion mechanisms of anaerobic cellulolytic species to cellulosic substrates have been identified to be mediated by (i) the cellulase complex (cellulosome) through the CBD, (ii) by glycosylated moieties of catalytic or non-catalytic cellulose binding proteins in the cell envelope, (iii) by the carbohydrate epitopes of the

bacterial glycocalyx and (iv) by fimbriae or other proteinaceous appendages. The actual strategies employed by individual species might be a combination of the above mechanisms as proven by finding on adherent rumen cellulolytic bacteria (Miron *et al*, 2001); however further research is needed to extend this knowledge to other naturally occurring anaerobic bacteria.
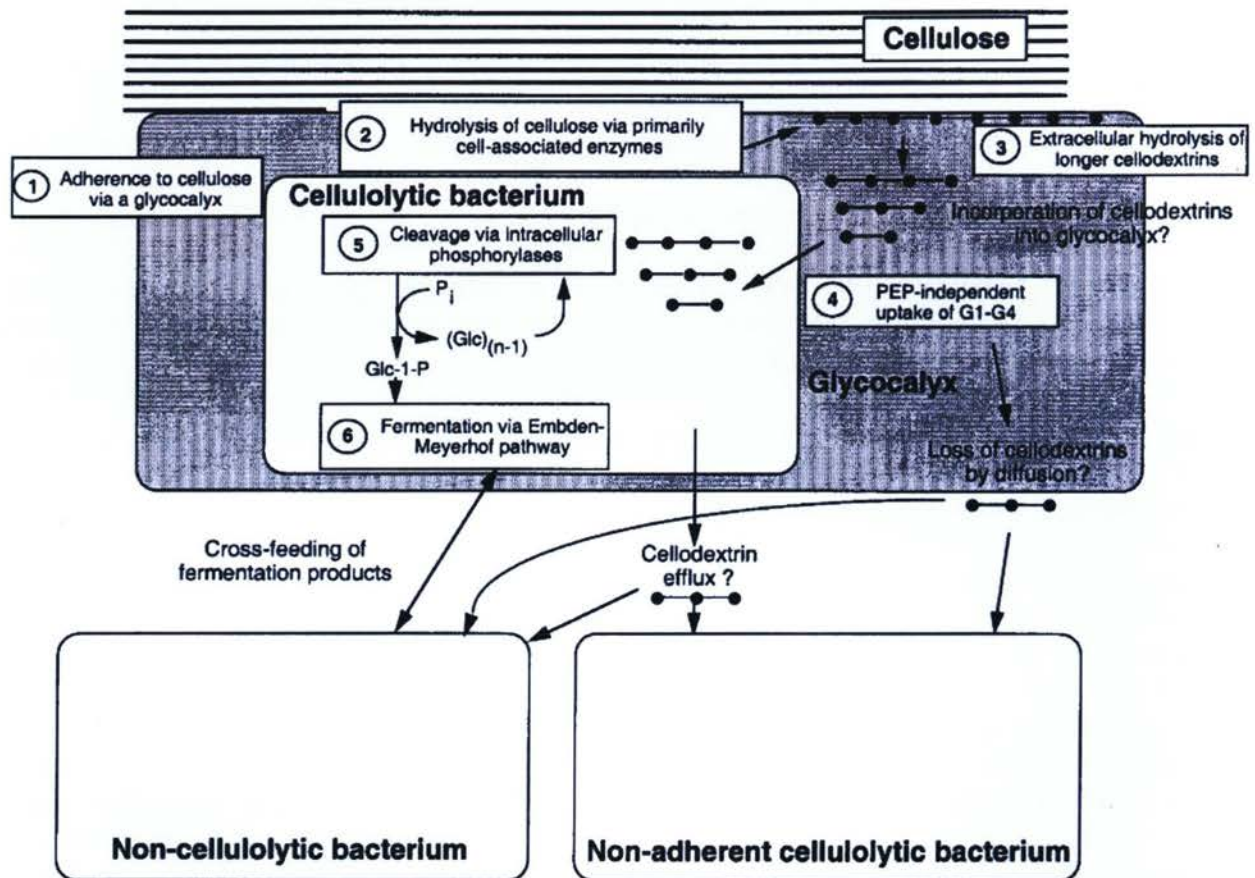
Figure 1.5 Schematic representation of cellulolytic bacterium glycocalyx-mediated adherence to cellulose. Adopted from Lynd *et al* 2002.

Adhesion to substrate, especially mediated by the glycocalyx (Figure 1.5), and the formation of a cellulose-enzyme-microbe (CEM) ternary complex has been theorized to provide a series of advantages to the cellulolytic organism which include: enzyme concentration at the cellulose surface, fast sequestration of the oligomeric

substrate hydrolysis products, protection from predation (grazing protozoa) or bacteriaphage attack and in the case of ruminal bacteria, protection for rumen proteases (Lynd *et al*, 2002). The benefits seem to outweigh the extra energy demand for the biosysthesis of glycocalyx precursors and of cellulose binding factors, which for example in the case of the nonprotein fraction of EPS has been proven to represent ≤4% of the total anabolic ATP expenditure of the anaerobic bacterium. (Weimer *et al*, 2006).

1.4. *Clostridium thermocellum* as a model cellulolytic organisms

Clostridium thermocellum, one of the best characterized thermophilic anaerobic bacterium capable of complete cellulolysis, was first described in 1926 in samples of horse manure (Viljoen *et al*, 1926) and it took nearly another 25 years before it was isolated in pure culture (McBee, 1950) and another four years for a more complete description of the cell characteristics (McBee, 1954). These early studies described the vegetative cells as straight or curved rods of 0.6 - 0.7 µm by 2.5 - 3.5 µm, that usually occur as individuals but can form long chains in fluid media. The spores were described to be 1.2 – 1.6 µm in size, oval and terminal, causing swelling of the cell. Later descriptions, found spore size and prevalence to be dependent on the type of substrate utilized, with abundant large spore formation during optimal growth on cellulose and fewer smaller spores while grown on glucose as the sole carbon source. Spore formation was linked with a pH drop under 6.4 or prolonged decrease of temperature

21

below 45°C, and quite commonly large cells (of up to 40 μm in length) with terminal endospores where observed (Freier *et al*, 1988). Like other strict anaerobes in the phylum Firmicutes, the bacterium is classified as a low G+C gram positive, however it exhibits a negative gram-reaction as explained by the variability in gram-staining reaction (Wiegel, 1981). The organism has an optimum growth temperature of around 60°C and an optimum pH range between 6.7 and 7.0. The minimum doubling time on cellulose, in optimal condition, has been reported to be 6 hours and on cellobiose a shorter 2.8 hours (Freier *et al*, 1988).

During hydrolysis of cellulose, *Clostridium thermocellum* is known to produce a yellow affinity substance (YAS) which readily adsorbs into cellulose. Its exact chemical structure is yet unknown but is believed to be similar to a carotenoid-like compound with an approximate MW of 1050 to 1300. The substance is easily oxidized in the presence of oxygen with loss of color. Most importantly, the YAS was suggested to not only facilitate the binding of cellulase to the substrate but also to serve as a signal mechanism for cellulose presence to the bacterium (Ljungdahl *et al*, 1983). More recent work on cellulolytic cultures of *Ruminococcus flavefaciens* has found the production of a YAS with strong affinity for microcrystalline cellulose and with observed properties very similar to the yellow substance in *C. thermocellum* (Kopečný and Hadrova, 1997). The binding affinity to cellulose was observed in the pH range of 5 to 8 and at temperatures from 10°C to 60°C and through HPLC the yellow compound was proven to have high affinity for two tested ruminococcal cellulases (endoglucanases and cellobiohydrolases). The cellulases were found to have higher adsorption to the cellulose-YAS complex than

to the untreated microcrystalline cellulose which also correlated to an increase in their activity.

Clostridium thermocellum is widespread in nature, usually populating organic material in decomposition. It was isolated from both natural and artificial environments such as soils, compost, animal feces, sewage digestion sludge, and surface geothermal features (e.g. hot springs) where it was thought to be involved in plant cell wall hydrolysis and the supply of oligomeric carbohydrates and end products of fermentation to other members of the microbial community (Lynd *et al*, 2006). The bacterium has a limited spectrum of substrate utilization with the most common carbon source being cellulose or pre-treated cellulosic biomass (Lynd *et al*, 1989) and its hydrolytic products (cellobiose and cellodextrins). Some strains have been reported to grown on additional carbohydrates such as glucose, fructose and sorbitol (Strobel, 1995; Demain *et al*, 2005) where growth usually requires a long period of adaptation to the non-cellulosic substrate and the induction of monomeric sugar degrading enzymes. Furthermore, microbial growth rates were found to be higher on cellobiose than on glucose and even more expressed on cultures grown on cellotetraose. Also it was reported that at slow growth rates, the glucose-grown cells had a fourfold increased maintenance energy than the cells grown on cellobiose (Strobel, 1995). The proposition that the bacterium benefits from increased chain length is supported by energetic studies on ATP balance (generation and consumption) during fermentation of ß-glucans by *C. thermocellum* (Zhang and Lynd, 2005). An ATP balance equation (G_{ATP}^{P-T}) was generated, which corresponded to the net difference of ATP gain from phosphorolytic cleavage of cellodextrins less the ATP required for transport (units of moles ATP/mole hexose).

Experimental determinations of the ATP balance in chemostats fed with cellodextrins of varying chain length led to the empirical prediction that G_{ATP}^{P-T} = (n-2)/n (where n is the chain length). For cultures grown on cellulose, the energy balance was reported to be 0.52 ± 0.6, which solved for a mean cellodextrin chain length of n = 4.2 ± 0.46. This implies that the products of cellulose solubilization have an average degree of polymerization equal to four. These finding were also supported by results from ^{14}C labeling studies on cellulose and cellobiose where the radioactivity of intracellular cellodextrins was found to indicate a mean-chain length of four for cultures exposed to labeled cellulose (Zhang and Lynd, 2005). When rates of phosphorolytic cleavage of ß-glucan substrates were compared to rates of hydrolytic cleavage it was reported that the former has up to a 20-fold increased prevalence than the latter when cells were grown on G2 and G5 glucans (Zhang and Lynd, 2004). Both reactions occur intracellularly but the phosphorolytic reaction is important from a bioenergetic perspective because it represents an ATP generation route for organisms specialized for growth on ß-glucans. Coupled with the considerations mentioned above, it is evident that for organisms growing on cellulose, bioenergetic benefits are higher with the increase in cellodextrin chain length due to the combined effect of ATP generation from phosphorolytic cleavage and energy savings from ATP expenditure per hexose in membrane transport. These benefits are believed to greatly overcome the ATP required for cellulase synthesis for growth on cellulose as compared to growth on cellobiose (Lynd et al, 2006), with figures on ATP expenditure for biosynthesis going for 20% on cellulases and the balance on cell synthesis (Zhang and Lynd, 2004).

The products of cellulose hydrolysis (cellobiose and cellodextrins) are taken up intracellularly by substrate transport mechanisms via an adenosine-binding cassette system (Lynd *et al*, 2002) and metabolized to glucose-1-phosphate (G-1-P) by the ATP-independent activity of intracellular cellobiose- and cellodextrin phosphorylases. G-1-P is then converted to glucose-6-phosphate (also the first product from glucose catabolism) which enters the Embden-Meyerhof fermentation pathway to yield pyruvic acid. This intermediate is converted to a mixture of end products which include ethanol, acetic acid, lactic acid, H_2 and CO_2 (Lynd *et al*, 2006).

Clostridium thermocellum produces an extracellular macromolecular multi-enzyme complex, defined as cellulosome (Figure 1.6), which combines all its components in an intermolecular synergistic manner to promote an efficient hydrolysis of the substrate. The cellulosome backbone is a non-catalytic complex, the scaffoldin (Ct-CipA), containing nine type-I cohesion domains, a family IIIa carbohydrate binding module (CBM IIIa) and a type-II dockering domain at the C-terminus. The enzymatic subunits in the cellulosome are complex proteins themselves, containing one or more catalytic domains in the form of glycosyl hydrolases, which include cellulases, hemicellulases (xylanase, mannose, chitinase and lichenase), and carbohydrate esterases (Bayer et al 1998). It is worth mentioning that the hydrolytic products of hemicellulolytic activity are not utilized by *C. thermocellum* and it has been suggested that these enzymes' function are to facilitate a better exposure of cellulose in the complex cell wall or these cellulosomal elements are the co-evolution result of the symbiotic interaction in mixed cellulolytic communities (Lynd *et al*, 2006).
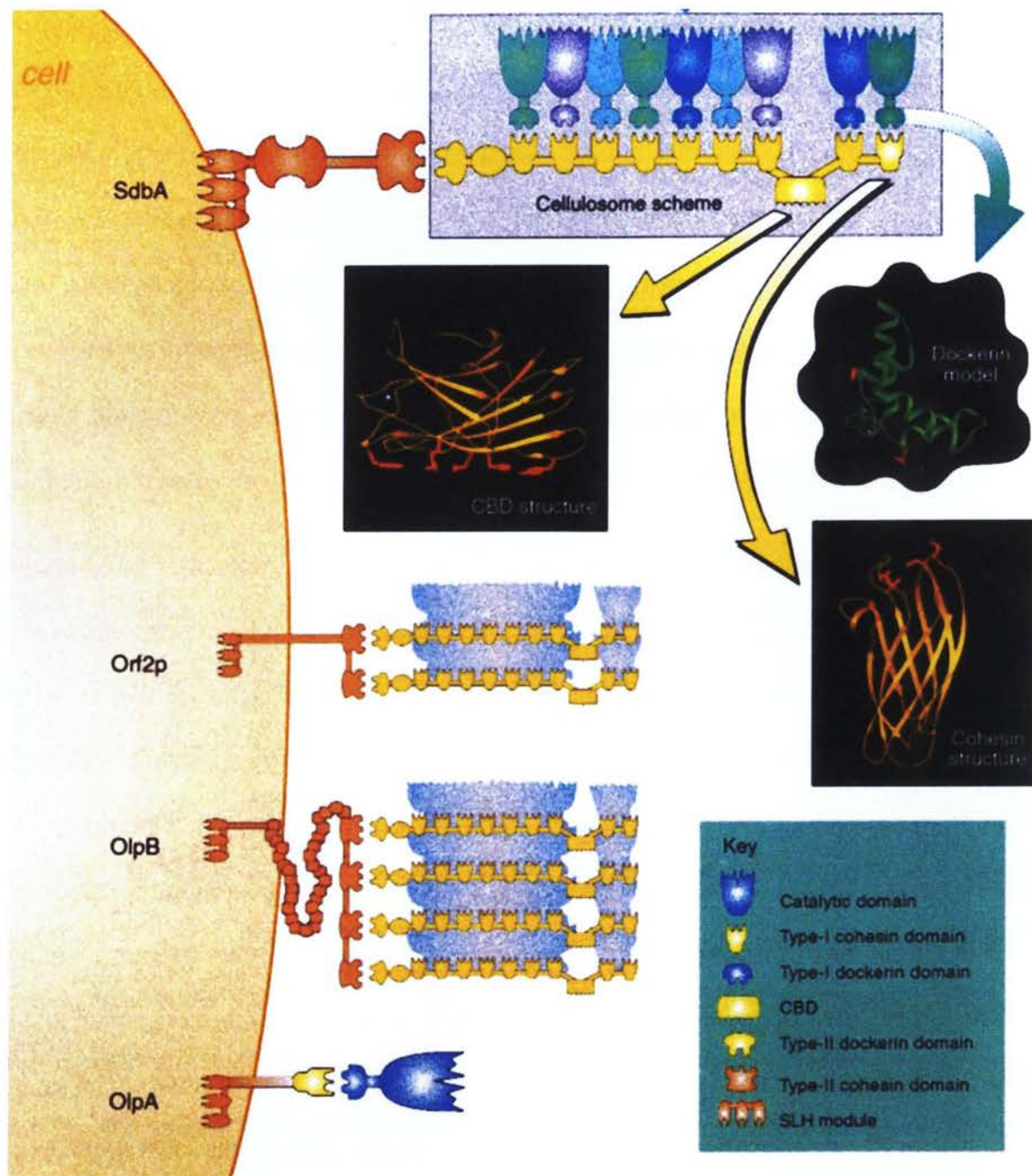
Figure 1.6 Schematic representation of the cellulosome organization and attachment to the *C. thermocellum* cell surface. Adopted from Bayer *et al*, 1998.

The non-catalytic portion of the enzymatic units contain a type-I dockerin domain

which anchors it to the type-I cohesion domain of the scaffoldin. Some cellulosomal

enzymes can also present CBMs as part of their structure, but they differ from the strongly binding CBM IIIa of the scaffoldin subunit which is believed to be primarily responsible for interactions with crystalline cellulose (Schwarz, 2001). The scaffoldin subunits, bearing the enzymatic elements, are coupled in modules of one, two or four to the type-II cohesive domains of the cell-wall binding proteins SdbA, Orf2P, and OlpB respectively.   These proteins are believed to adhere to the cell envelope by three consecutive SLH anchoring domains at their C-terminus (Bayer *et al*, 1998).

In *C. thermocellum*, polycellulosomal structures have been demonstrated to exist at the cell surface forming multiple protuberances (Bayer and Lamed, 1986). Electron micrographs of anti-body labeled cells adherent to cellululose, indicate the protuberances undergo structural conformations to form fibrous contact corridors connecting the cell and the substrate at distances of over 500 nm (this being the only reference of measured cell-substrate gap in the literature). These protracted protuberances were proposed to help in channeling the product of cellulose hydrolysis to the cell to be taken up via the appropriate transport mechanisms (Bayer *et al*, 1998), potentially providing a competitive advantage for the adherent bacterium cells.

CHAPTER 2. METHODOLOGY

2.1. Materials and Microorganisms

Source of Chemicals and Materials. All chemicals were reagent grade or molecular grade as indicated and were obtained from VWR (Mississauga, ON.), Sigma-Aldrich (Oakville, ON.) and Invitrogen (Carlsbad, CA.) unless otherwise indicated. Materials used for batch and continuous-flow microbial systems were obtained from Cole-Parmer (Montreal, QC.) unless stated otherwise.

Microorganisms. *Clostridium thermocellum* ATCC 27405 was kindly provided by Dr. Paul Weimer (University of Wisconsin) and was maintained in batch culture vials stored at 4°C under anaerobic conditions. Working batch cultures were grown in a modified RM medium (Ozkan *et al*, 2001) containing Avicel PH101 as cellulosic source. Working continuous-flow cultures were grown in modified RM media without Avicel and with commercial cotton as solid cellulosic substrate. *Saccharomyces cerevisiae* VIN13 was provided by Desire Barnard (University of Stellenbosch) and was maintained in Yeast-Peptone-Dextrose (YPD) medium (Gutiérrez-Lomelí *et al*, 2008). Continuous-flow yeast systems were grown in a synthetic minimal medium with Yeast Nitrogen Base (1.7g/L) without amino-acids Difco #0919-15 (Fisher Scientific, Pittsburgh, PA.) and commercial cotton was used as carbon source.

Growth medium for batch cultures. RM medium (Ozkan *et al*, 2001; Tsoi *et al*, 1987), a complex synthetic growth medium, using potassium phosphate to provide the pH

buffering, was prepared for batch culture growth following a modified Hungate technique (Hungate, 1969; Hungate, 1950), with final concentrations as shown in Table 2.1. The components, consisting of urea, KH_2PO_4, K_2HPO_4, yeast extract and Avicel, and the 50-fold concentrated Resazurin stock solution were added to a master-mix solution. Equal volumes were dispensed in serum vials, which were then sealed with butyl-rubber stoppers and aluminum crimps. A system consisting of tubing, a splitting manifold and needles, were used to evacuate the air headspace in each vial before flushing with Nitrogen grade 4.8 (BOC Gasses, Mississauga, Canada) at 15 second intervals for 3 minutes. Vials were then sterilized in an autoclave for 20 minutes. The L-cysteine hydrochloride monohydrate solution was prepared 10-fold concentrated in larger serum bottles with distilled water containing 0.002% Resazurin (optional). The vial was crimp-sealed and the air headspace was replaced with N_2 as described above followed by sterilization for 20 minutes. The mineral solution, containing $MgCl_2$ $6H_2O$, $CaCl_2$ $2H_2O$ and $FeSO_4$ $7H_2O$, was prepared 100-fold concentrated with ultrapure deionized water (model Milli-Q Advantage A10 Water purification system, Millipore Corp., Billerica, MA, USA) and then sterilized with a 0.2µm filter (Fisherbrand, Canada.).

YPD medium, a common synthetic media used for optimal *S. cerevisiae* growth, was prepared with final concentrations as shown in Table 2.2. Bacto-peptone and yeast extract were mixed in water and autoclaved for 20 minutes. The solution was allowed to cool to approximately 55°C and then a sterile glucose solution was added to bring the media to the correct final volume. From this mix, equal volumes were transferred to pre-sterilized test tubes.

Table 2.1 Composition of RM medium for batch cultures of *C. thermocellum*

Ingredient	Stock (g/L)	Final (g/L)
Urea: CH_4N_2O	(crystals)	2
Potassium Phosphate monobasic: KH_2PO_4	(crystals)	2
Potassium Phosphate dibasic: K_2HPO_4	(crystals)	3
Yeast extract	(powder)	2
Avicel	(crystals)	5
Reducing agent and Redox indicator Sols.		
L-Cysteine Hydrochloride monohydrate: $C_3H_7NO_2S * HCl * H_2O$	10	1
Resazurin, Sodium salt: $C_{12}H_6NNaO_4$	0.1	0.002
Mineral Solution		
Magnesium Chloride hexahydrate: $MgCl_2\ 6H_2O$	20	0.2
Calcium Chloride dihydrate: $CaCl_2\ 2H_2O$	5	0.05
Ferrous Sulfate heptahydrate: $FeSO_4\ 7H_2O$	0.25	0.0025

Table 2.2 Composition of YPD medium for batch cutures of *S. cerevisiae*

Ingredient	Stock (w/v)	Final (w/v)
Bacto-peptone	(powder)	2%
Yeast extract	(powder)	1%
Glucose: $C_6H_{12}O_6$	40%	2%

Medium for continuous-flow cultures. RM media lacking cellulose – Avicel PH101, was prepared with final concentrations as shown in Table 2.3. The solid components, consisting of urea, yeast extract and the buffer elements (two potassium phosphate bases) were mixed in ultrapure deionized water and the 50-fold concentrated Resazurin solution was added before autoclaving for 20 minutes. Double autoclaving of this mixture ensures better oxygen reduction in the solution but it is entirely optional. The medium flask container and the rubber cap element will be discussed below in Section 2.3.1.1. After sterilization, the solution was cooled down by purging Nitrogen gas (grade 4.8) through a 0.2µm filter into the media flask for 90 minutes. The 100-fold concentrated mineral solution mix was prepared and sterilized as described above. Using sterile syringes and needles (BD 22G needle, Fisher Scientific, Canada) the solution of minerals was injected into the cooled media. L-cysteine hydrochloride monohydrate, prepared 30-fold concentrated as described previously, was added to the medium via syringe and needle (BD 18G needle, Fisher Scientific, Canada). The anaerobic medium can be sealed and stored at room temperature for up to 48 hours before use.

SD medium, a synthetic minimal media for *S. cerevisiae* growth, was prepared with no carbon source using final concentrations as shown in Table 2.4. The medium, containing Difco YNB, ammonium sulfate and the redox indicator – Resazurin, was autoclaved for 20 minutes and then cooled by purging with N_2 gas (grade 4.8). No reducing agent, such as L-cysteine HCl, was added.

Table 2.3 Composition of RM medium for continuous-flow cultures of *C. thermocellum*

Ingredient	Stock (g/L)	Final (g/L)
Urea: CH_4N_2O	(crystals)	2
Potassium Phosphate monobasic: KH_2PO_4	(crystals)	2
Potassium Phosphate dibasic: K_2HPO_4	(crystals)	3
Yeast extract	(powder)	2
Reducing agent and Redox indicator Sols.		
L-Cysteine Hydrochloride monohydrate: $C_3H_7NO_2S * HCl * H_2O$	30	1
Resazurin, Sodium salt: $C_{12}H_6NNaO_4$	0.1	0.002
Mineral Solution		
Magnesium Chloride hexahydrate: $MgCl_2\ 6H_2O$	20	0.2
Calcium Chloride dihydrate: $CaCl_2\ 2H_2O$	5	0.05
Ferrous Sulfate heptahydrate: $FeSO_4\ 7H_2O$	0.25	0.0025

Table 2.4 Composition of SD medium for continuous-flow cultures of *S. cerevisiae*

Ingredient	Stock (g/L)	Final (g/L)
Yeast nitrogen base (YNB) without aminoacids (Difco 0919-15)	(powder)	1.7
Ammonium Sulfate: $(NH_4)_2SO_4$	(powder)	5
Redox indicator sol.		
Resazurin, Sodium salt: $C_{12}H_6NNaO_4$	0.1	0.002

2.2. **Batch culture growth**

Batch culture of *Clostridium thermocellum*. The bacteria were grown in batch cultures to serve as fresh source for inoculation, long term stock culture and for experiments where the interaction between *C. thermocellum* and cellulose (Avicel) was investigated *in-vitro* using microscopy. *C. thermocellum* cultures were transferred from stock (5% v/v inoculums) to 20mL serum vials (for experiments) or 100 mL serum bottles (for storage at 4°C) containing half their volume with RM media. Avicel crystals of 50µm average size served as the cellulosic carbon source at a concentration of 5g/L. The inoculations were made under normal or N_2 atmosphere via sterile syringes and needles (BD 25G needle, Fisher Scientific, Canada) and the cultures were incubated without shaking at 60°C. For re-inoculations of batch cultures or the inoculation of flow cells, samples were removed via syringes and 25G needles under normal or N_2 atmosphere during incubation periods or from 4°C storage cultures. For microscopy experiments on batch cultures incubated at 60°C, samples were removed from the cultures under normal atmosphere only.

Batch culture of *S. cerevisiae* vin13. The yeast strain was grown in batch culture to serve as inoculum source for flow cell experiments. Stock cultures of *S. cerevisiae* were transferred (5% v/v inoculum) into test tubes containing 5mL YPD medium and incubated with shaking in a heating shaker (model MaxQ4000, Barnstead Int. Lab-line, Dubuque, IA, USA) set at 30°C and 300rpm. Samples were collected with syringes and 25G needles during incubation for the inoculation of flow cells.

2.3. **Continuous-flow culture**

Continuous-flow experiments were carried out under normal atmosphere and under a N_2 atmosphere. Growth in flow cells kept under a nitrogen atmosphere was possible with the use of an anaerobic cabinet equipped with a heating incubator (Type B Vinyl Anaerobic Chamber, Coy Lab. Prod., Grass Lake, MI, United States) and was suited for experiments where a one-time culture evaluation was desired or where sample collection and flow cell analysis over time was not limited by the confined chamber space. For experiments where the interaction between *C. thermocellum* and its substrate was investigated *in-situ* using the confocal laser scanning microscope (CLSM), flow cells were used in the anaerobic chamber under a N_2 atmosphere.

Growth in flow cells kept under normal atmosphere was possible with the use of a newly developed continuous-flow system design (Section 2.3.1.2) and was suited for experiments where sample collection and flow cell measurements required the use of devices not fitted for an anaerobic chamber. For experiments where the *C. thermocellum* flow cell effluent was measured for dissolved carbon dioxide, total carbohydrate and total non-attached cell counts, the cultures were grown in anaerobic systems kept under a normal atmosphere. For control experiments where the relation between *S. cereviasiae* and a solid cellulosic substrate was investigated *in-situ*, the flow cells were kept in a closed continuous-flow system (Section 2.3.2) under a normal atmosphere.

2.3.1. Continuous-flow cultures of *C. thermocellum*.

The concept of continuous flow cells, developed elsewhere (Wolfaardt *et al*, 1994), was used with multiple modified chamber designs (Figure 2.1) where solid cellulose, in the form on commercially available cotton, was immobilized inside flow chambers and served as the single, insoluble, source of cellulosic carbon for *C. thermocellum* growth.
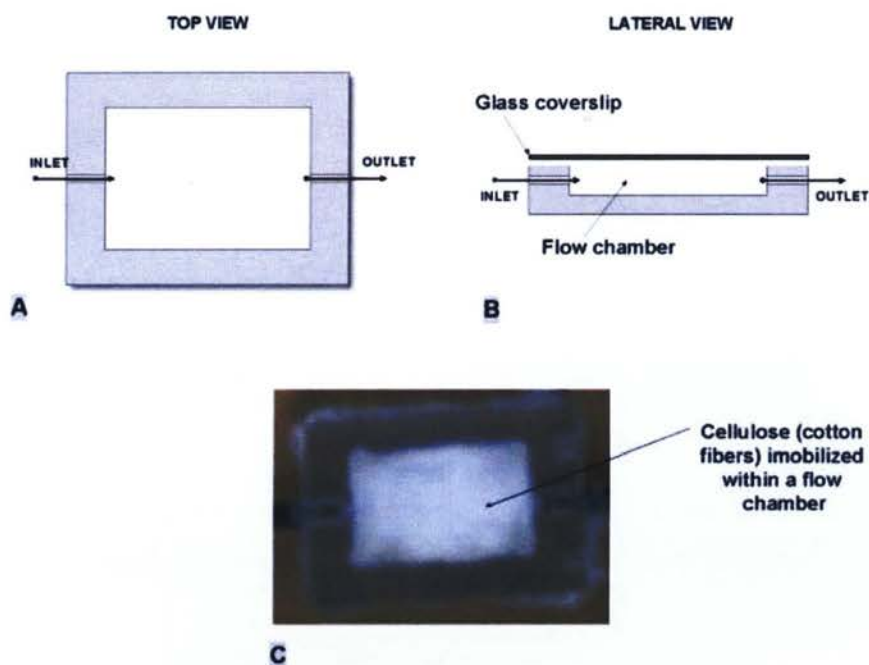
Figure 2.1 Schematic flow cell design showing top view (A) and lateral view (B); and an image of a typical acrylic glass flow cell construct (C) used for continuous-flow cultures of anaerobic, thermophile *Clostridium thermocellum*

Stock cultures or incubated cultures of *C. thermocellum* were transferred (10%-30% v/v inoculums) into the flow chamber via sterile syringes and 25G needles and the medium was kept stationary for 60 minutes to allow potential cell-surface interactions to occur. Thereafter, flow was initiated and maintained at constant rates for the duration of the experiment at 60°C.

2.3.1.1. **Continuous-flow systems under a N$_2$ atmosphere**

RM media was prepared as described above and stored inside or outside of the anaerobic chamber for up to 48 hours to allow the photocatalytic reduction of oxygen by L-cysteine HCl. Exposure of media to a higher light intensity (Fukushima *et al*, 2003) hastened the reduction time. The use of a special cap design (Figure 2.2) ensured the aseptic preparation and storage of media without the need of a ambient N$_2$ atmosphere.
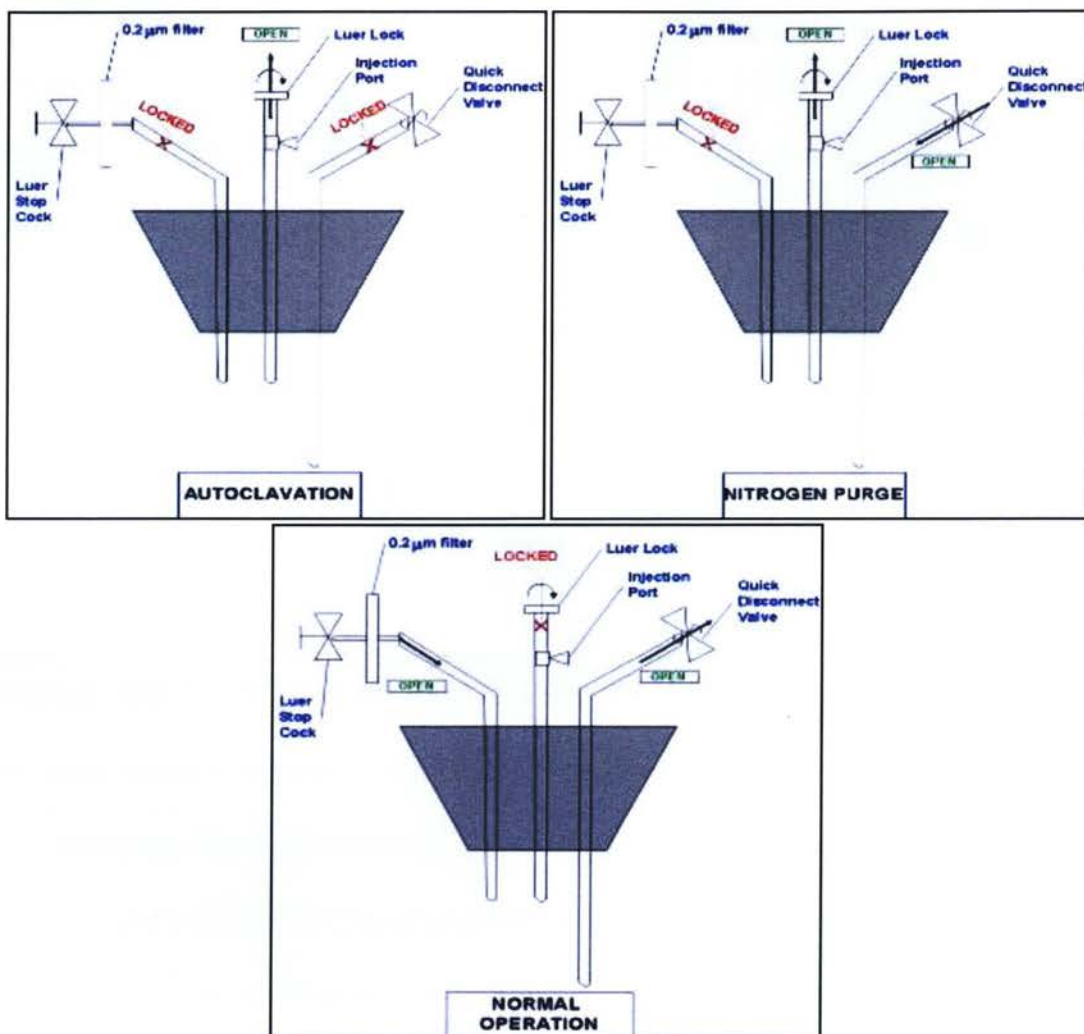
Figure 2.2 Rubber cap design for anaerobic media preparation and storage under normal or N$_2$ atmosphere. The diagrams show the open and locked position of the three ports during media autoclaving, nitrogen purging and normal operation with a continuous-flow system.

Reactor design. The continuous-flow system (see Figure 2.3) was composed of an RM medium container, silicone tubing (0.188 x 0.313 x 0.063 in., I.D x O.D x Wall, VWR, Mississauga, ON, Canada), a flow cell, a peristaltic pump (Dynamax RP-1, Rainin Instrument Co., Emeryville, CA, United States), and an effluent waste container. The tubing system and the flow chamber were sterilized by pumping a 10% Sodium Hypochlorite solution (Bleaching agent) at approximately 40 mL/h for 30 to 60 minutes which was then washed out with sterile distilled water overnight at 10 mL/h.
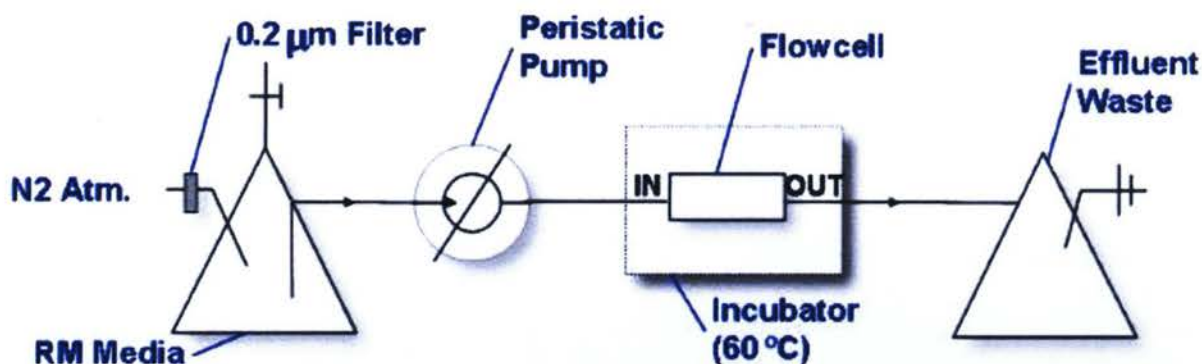
Figure 2.3 Schematic diagram of a continuous-flow system used under a N_2 atmosphere. Cellulose-free RM media is pumped via a tubing system through a flow cell containing the solid cellulosic substrate, where growth of anaerobic, thermophile *C. thermocellum* occurs.

Culture growth. The RM media was coupled with the tubing system and pumped in at 40mL/h for approximately two hours during which the flow chamber was moved inside the 60°C incubator (Model 2002, Coy Lab. Prod., U.S.) of the anaerobic cabinet unit. For inoculation, the medium flow was stopped; a *C. thermocellum* stock or incubated culture was transferred via syringe and 25G needle through the silicone tubing directly inside the flow chamber and the system was kept with no flow for 60 minutes. Normal operation was started with a medium flow set to 10mL/h. The cultures were used at various stages of growth ranging from 24 hours to 120 hours for microscopic

investigations. Sample preparation and staining procedures are detailed in Section 2.4.2.

2.3.1.2. **Continuous-flow systems under normal atmosphere.**

Under ambient atmosphere the system described above was modified to accommodate an oxygen-free medium source in a unidirectional flow system and a set of sample collection devices on the effluent side (Figure 2.4). To ensure pure culture conditions and to eliminate unwanted microbial contamination external ports were protected with 0.2 μm filters (not all shown in Figure 2.4).
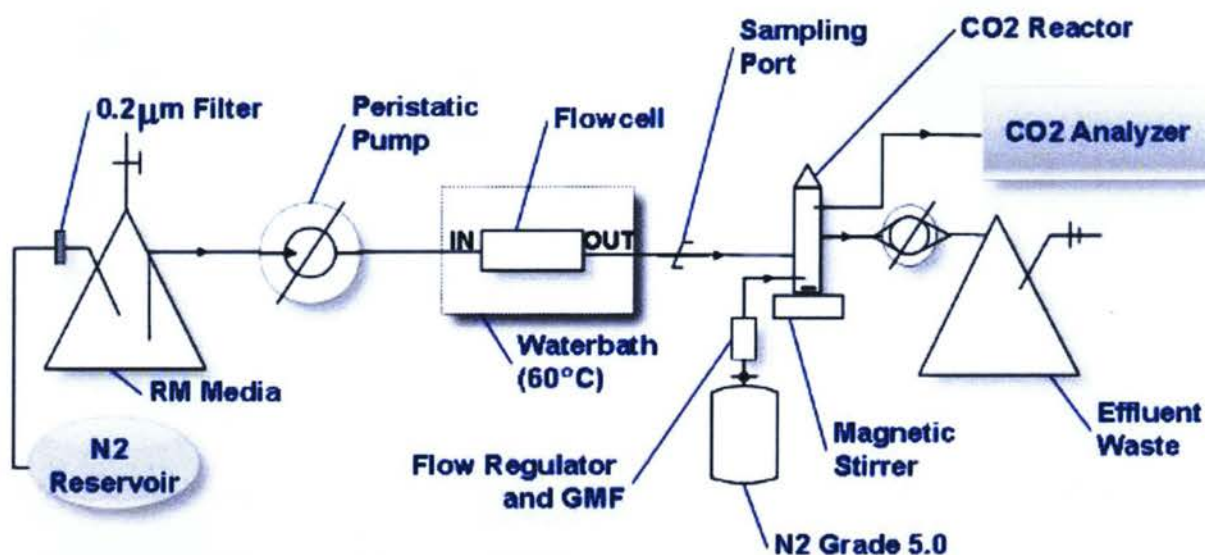
Figure 2.4 Schematic diagram of a continuous-flow system used under normal atmosphere for growth of anaerobic, thermophile, *C. thermocellum* cultures. A sampling port allows the aseptic collection of liquid effluent samples; and a "CO₂ exchange reactor" purged with N₂ gas and coupled to an infrared analyzer allows real-time measurements of dissolved CO₂ in the effluent. GFM – Gas Mass Flowmeter.

Reactor design. The continuous-flow system was composed of a N_2 grade 4.8 reservoir (typically a gas impermeable bag) fitted with valves for quick connect or.disconnect; an RM medium container, a peristaltic pump (Watson Marlow model

205S, Bredel Inc., Wilmington, MA, USA); a flow cell; a water bath (model Precisterm 5L, Rose Scientific Ltd., Canada) set at 60°C; an optional CO_2 exchange reactor and its accessories (see below); and an effluent waste container. Norprene tubing (size L/S 14 and size 16) was used for its low gas permeability ratings; and Tygon tubing (1/16 x 1/8 x 1/32 in., I.D. x O.D. x Wall, VWR, Canada) was used for the CO_2 reactor accessories and towards the effluent waste container.

The CO_2 exchange reactor (Figure 2.5) was made of a cylinder plastic body, equipped with a stir bar at the bottom, positioned on a magnetic stirrer plate. It received the flow cell effluent at a rate of 10 mL/h (or 1.5 rpm pump speed); while the liquid outflow was pumped out with two tubes, which ensured a constant liquid volume inside the reactor. A N_2 grade 5.0 gas cylinder, equipped with a sensitive gas flowmeter (Air/N_2 Thermal Gas Mass Flowmeter, 0 to 50 sccm, model GMF 17) and a manual flow controller unit (model type Mini Filter/Regulator), supplied the inflow of sweeper gas into the reactor, to sparge the liquid content at rates of 25 mL/min. The gas outflow was directly coupled to an infrared CO_2 gas analyzer (LI-820 CO_2 Analyzer, LI-COR Biosciences, Lincoln, ME, United States) and the data recorded in real time. The tubing and the flow chamber were sterilized and washed as detailed in the previous section.

Operation of continuous-flow system. The container with anaerobic medium was aseptically coupled to the flow cell system and to the N_2 reservoir and flow was initiated at 40 mL/h for up to two hours, during which the flow chamber was heated to 60°C immersed into the water bath. For inoculation, stock cultures of C. thermocellum were transferred via syringes and 25G needles through the Norprene tubing directly into the flow chamber and the pump was kept off for 60 minutes. Normal operation was

resumed with pump set to 1.5 rpm having a flow of 10 mL/h. Cultures were incubated at 60°C and grown for up to 6 days, during which carbon dioxide measurements were recorded at set intervals from the CO_2 exchange reactor; following these measurements, liquid samples were aseptically collected via a sampling port at the flow cell effluent side and processed or stored, as detailed in Section 2.6, for total carbohydrate content and for total non-attached cell counts.
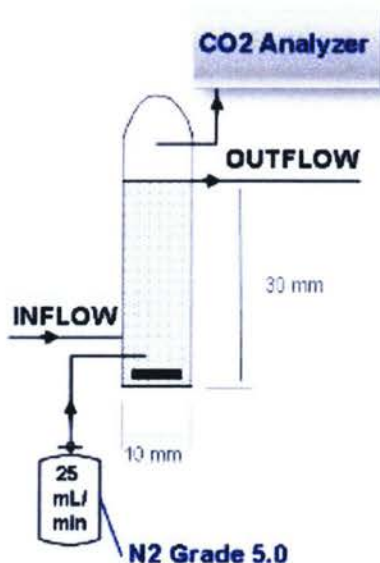
Figure 2.5 Schematic diagram of the CO_2 exchange reactor attached to the effluent side of *C. thermocellum* continuous-flow cultures.

2.3.2. Continuous-flow cultures of *S. cerevisiae*

Cultures of *S. cerevisiae* were grown as control specie in continuous-flow mode for experiments where the colonization behavior between cellulolytic and non-cellulolytic microorganisms was investigated.

Reactor design. The continuous-flow system consisted of an SD medium (Table 2.4) reservoir, a flow cell containing solid cellulose in the form of cotton fibers, a peristaltic pump (Watson Marlow model 205S), and Tygon tubing. It functioned in a closed loop design, where the flow cell effluent tubing was connected back to the media container (Figure 2.6). The set-up was run under a normal atmosphere and it was sterilized and washed as described in Section 2.3.1.1.
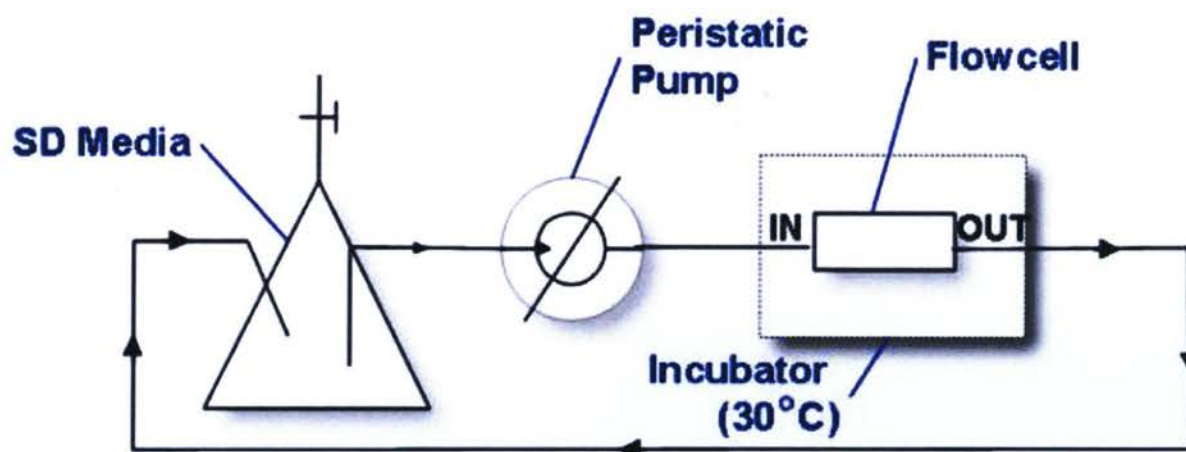
Figure 2.6. Schematic diagram of a continuous-flow system for growth of *S. cerevisiae* cultures.

Operation of continuous-flow system. After sterilization and overnight washing, the SD medium reservoir was coupled to the tubing system and flow was initiated at 40 mL/h for two hours. The pump was stopped and a cellulase mixture, Spezyme® (generously donated by Dr. Lee R. Lynd, Dartmouth College, NH) was injected directly into the flowcell. The enzyme cocktail (with glucanase, xylanase and ß-glucosidase activity) had a stock measured activity of 61FPU/mL and was used with a final activity of 15FPU/g cellulose into the flow cell. For inoculation, incubated cultures of *S. cerevisiae* were transferred (5% v/v inoculums) directly into the flow chamber and the system was

left without flow for 30 minutes. Flow was resumed at 10 mL/h and the culture was incubated at 30°C for 3 days. Staining procedures and sample preparation for microscopy investigations are detailed in Section 2.4.3.

2.4. Microscopy

Batch cultures of *C. thermocellum* were analyzed *in-vitro* with a Leica wide field epifluorescence microscope (model DM 5000B, Leica Microsystems, Canada). Continuous-flow cultures of *C. thermocellum* and *S. cerevisiae* were analyzed *in-situ* with a Zeiss confocal laser scanning microscope (model LSM 510, Carl Zeiss Canada Ltd.). Effluent samples of continuous-flow *C. thermocellum* cultures were analyzed for total non-attached cell counts with a Zeiss inverted fluorescence microscope (model Axiovert 200M, Carl Zeiss Canada Ltd.) as detailed in Section 2.5.3.

Stain stocks and the working solutions derived from them were prepared with ultrapure sterile deionized water as detailed in the following sections. Supplier product information sheet instructions were followed for storage and handling.

2.4.1. Epifluorescence microscopy of batch cultures of *C. thermocellum*

Batch sampling occurred after 24h and up to 96h of growth. Sample volumes of 100µL to 500µL were mixed with a single stain (Table 2.5) and incubated at room

temperature, protected from light, for 20 to 30 minutes. From this mixture 20µL-50µL were transferred via pipette on microscope slides with coverslips without fixation.

Table 2.5. Stain stocks and working volumes used with batch cultures of *C. thermocellum* in wide field epifluorescence microscopy (the solvent volume in the working solutions represents the total final volume of the mixture)

Stain name	Stock conc.	Working sol. Preparation	Target	Use
4',6-Diamidino-2-phenylindole (DAPI)	2.5 mg/mL	100µL / 1mL H_2O	dsDNA	40µL/1mL Sample
Acridine Orange (AO)	0.25 mg/mL	10µL / 1mL H_2O	dsDNA & ssDNAssRNA	100µL/1mL Sample
Ethidium Bromide (EtBr)	10mg/mL	2-10µL / 1mL H_2O	dsDNA	100µL/1mL Sample

Slides were immediately investigated with the corresponding microscope filter settings and with the 63x1.4 oil immersion Plan-Apochromat objective lenses. Results were saved as image files, which were processed post-acquisition.

2.4.2. Confocal laser scanning microscopy on continuous-flow cultures of *C. thermocellum*

Staining protocols and sample preparation. Stain stocks and fresh working solutions were prepared as detailed in Table 2.6. The peristaltic pump flow was stopped and

volumes of 100μL to 1000μL of stain working solutions were transferred very slowly via 25G needles directly into the flow cell.

Table 2.6. List of stain stocks and the working volumes used on continuous-flow cultures of *C. thermocellum* in confocal laser scanning microscopy (final volumes of the working solutions are represented as the solvent volume)

Stain name	Stock conc.	Working sol. Preparation	Target
SYTO 9	3.34 mM	2-5μL / 1mL H_2O	Nucleic acids
Propidium iodide	20 mM	2μL / 1mL H_2O	Nucleic acids
FM 1-43	1 mg/mL	4-20μL / 1mL H_2O	Cell membrane (outer leaflet)
FM 4-64	2 mg/mL	4-20μL / 1mL H_2O	Cell membrane (outer leaflet)
Conjugated Lectins			
ConA-FITC & TRITC			α-glucose & α-mannose
PSA-FITC			α-mannose
DBA-FITC	1 mg/mL	4-20μL / 1mL H_2O	N-Acetyl Galactosamine
PNA-FITC			Galactose
UEA-FITC			Fucose
LEA-FITC			N-Acetyl Glucosamine
WGA-TRITC	5 mg/mL	1-4μL / 1mL H_2O	N-Acetyl Glucosamine
Acridine Orange (AO)	0.25 mg/mL	10μL / 1 mL H_2O	Nucleic acids
Ethidium Bromide (EtBr)	10 mg/mL	2-10μL / 1 mL H_2O	Nucleic acids
Nile Red	1 mg/mL	100μL / 1 mL H_2O	Intracellular lipids

The amount of stain injected was dependent on the flow chamber size and equaled a minimum of a quarter of its volume. The working solutions were tested across

the range of concentrations provided in Table 2.6, but typically a middle range value was used. All the stains were tested separately and in combination of two or more. A typical combination of two consisted of a nucleic acid stain supplemented with a secondary stain targeted against carbohydrates, lipids or proteins. Conjugated lectins were tested individually, coupled with a nucleic acid fluorophore (as the case of Concanavalin A or Wheat germ agglutinin) or in cocktails or five, six or seven lectins. Following stain addition, the flow cell was incubated at normal room temperature, protected from light, for 15 to 20 minutes. Media flow was then resumed at normal rates for 15 minutes to wash out unbound, excess stain. The flow cell was removed from the continuous-flow system having the inflow and outflow sealed off to maintain a fully anaerobic, stationary, hydrated flow chamber environment.

Microscopy protocols. For imaging, the flow cell was immobilized on the CLSM stage and results were recorded as raw data files for later image analysis (see Section 2.6). Depending on the fluorophore or the combination of fluorophores applied, the sample was excited at 488nm/514nm (Argon laser), 543 nm (HeNe laser) or 633nm (HeNe laser) through the thin glass cover slip of the flow cell. That design allowed the non-invasive imaging of the sealed anaerobic culture where the emission fluorescence was captured with a 63x1.2 water immersion C-Apochromat objective. In accordance to the employed fluorophores' spectral characteristics, the detection filters (perpendicular optical elements) used were selected from the following range: band pass (BP) 505-530; BP 500-550; BP 560-615; long pass (LP) 505; LP 560 and LP 650. Based on the excitation source and the filter selection, the oblique elements (main and secondary dichroic beamsplitters; corrective plates) in the optical path were set as per instructions

of the LSM 510 user manual. For samples stained with multiple fluorophores where overlapped excitation lasers with detection filters, or where multi-channel cross-talk was theoretically possible, the microscope configuration was set up in the multi-track mode.

Digital data was captured with the LSM 5 Image software as single images or as stacks of optical sections in the xy plane along the z-axis (referred to as z-stack). With the highest magnification objective and the optimal pinhole settings, the highest scaling (resolution) achieved along the x:y:z axes was 0.14µm:0.14µm:0.44µm. The use of glass and acrylic glass in the flow cell design, which was permissive to laser light penetration, allowed the capture of transmitted light images concurrently with the fluorescence images. This feature was used as focusing aid or in identifying non-fluorescent sample elements.

2.4.3. Confocal laser scanning microscopy on continuous-flow cultures of *S. cerevisiae*

Control samples of *S. cerevisiae* were prepared and visualized correspondingly with the procedures outlined above. The stain of choice was ethidium bromide prepared in stock and working solution as shown in Table 2.6. Raw data captured was later used in image analysis.

2.5. Measurements in effluent of *C. thermocellum* continuous-flow cultures.

Sample collection and measurements in continuous-flow culture effluent occurred at time zero, just before flow cell inoculation and referred to as media blank, and then every 24 hours after chamber inoculation for up to 6 days. Carbon dioxide measurements were performed before liquid sampling in all experiments, without changing of flow rates.

2.5.1. Carbon Dioxide measurements

The CO_2 exchange reactor was coupled to the N_2 gas input line and to the LI-820 gas analyzer (Figure 2.4) and inert gas was sparged through the reactor's liquid volume, which remained constant at 2.35 mL. The gas analyzer was programmed to record and save the CO_2 readings at 2 second intervals in the ppm range, and to plot the concentration values in a scale from 0 to 2000 ppm. With very stable volumetric flow control of the inert N_2 sparging, fluctuation in the recorded CO_2 values stayed within ±0.1 ppm. After approximately 60 minutes of sparging, the carbon dioxide measurement typically reached a stable value and arbitrarily at minute 90, the CO_2 concentration was recorded as a single measurement. Concurrently, the real-time plot of carbon dioxide concentrations within the 90 minutes of run-time was saved as a .bmp image file.

2.5.2. Total carbohydrates measurements

Flow cell effluent samples were aseptically collected in duplicate through a collection port (see Figure 2.4). They were collected at normal pump flow rates (10 mL/h) over precisely 8 minutes yielding a volume of 1.3mL effluent. The samples were then passed through a 0.2μm filter to eliminate cells and cellulosic fragments and stored at -20°C for later analysis of total carbohydrate by the Phenol-Sulfuric acid assay (Gerhardt et al 1994). The phenol colorimetric reaction with simple sugars was quantified by absorption readings at 488nm. Sample readings were run against a standard curve prepared with glucose in the range of 3.33μg/mL to 13.33μg/mL. Due to the effects of the redox indicator on absorbance readings, the standards were prepared with 0.02% Resazurin solution. Special acid resistant cuvettes were used (Brand UV-Cuvettes, Brandtech Scientific Inc, Essex, CT. United States). The assay is estimating the total amount of simple sugars and their polymers in the sample.

2.5.3. Total non-attached cell counts

Effluent samples were collected following the procedure outlined above. However, collected samples were immediately processed for total (live and dead) cell counts using an adapted epifluorescence direct enumeration technique (Kepner and Pratt, 1994; Massana et al, 1997). From a fresh sample serial dilutions were prepared in duplicate with a 10^{-1} and a 10^{-2} factor to a final volume of 900μL and 1000μL respectively. The dilutions were prepared in 850μL of 0.9% NaCl premixed with 50μL of 0.25mg/mL DAPI. The remaining volumes of undiluted samples were not used for the

rest of the procedure. The diluted samples were then incubated at room temperature, protected from light for 20 minutes, followed by transfer into a filter unit (model 25mm filter holders, No. 5 stopper , VWR, Canada) and very gently vacuum filtered through dark polycarbonate membrane filters (model Nucleopore Polycarbonate Membrane Filters, Black, Whatman, VWR, Canada). The funnel cap holds 25 mm filters but the internal working filtration area has a 15 mm diameter (see Figure 2.7) thus uniformly distributing the sample content over 176.6mm^2.
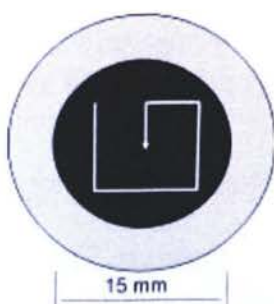
Figure 2.7 Schematic design of the Nuclepore polycarbonate filter showing the sample distribution area (darker zone) and the microscopy scanning pattern (white arrow).

Slides were immediately examined under fluorescence excitation on a Zeiss inverted fluorescence microscope using oil immersion with a 63x1.4 Plan-Apochromat objective. The polycarbonate membranes were pre-stained black to reduce background fluorescence and provided a high contrast with the DAPI stained bacterial cells. Images were captured as uncompressed .tiff files following the scanning pattern indicated in Figure 2.7 and a total of 30 fields were saved per sample. The microscope field size was of 225μm by 280μm thus bringing the total area counted per sample to 1.89mm^2. Only sample dilutions that contained between 20 and 200 cells per field were

considered for counting thus establishing a minimum of 600 cells counted per sample to an upward of 6000 cells per sample.

2.6. Image Analysis

Epifluorescence microscopy results of *C. thermocellum* batch cultures were saved with Adobe Photoshop CS (camera capture plug-in for Leica) as uncompressed .tiff image files and processed with Irfanview and Paint.NET software for brightness and color enhancement, resizing and cropping and file format compression.

Fluorescence microscopy results of total non-attached cells in *C. thermocellum* flow cell effluent were saved with Northern Eclipse software as uncompressed .tiff image files. Post acquisition, the "Cell counter" plug-in of ImageJ software was used to manually process the number of cells within three groups: normal cells, dividing cells and sporulated cells.

Laser scanning microscopy results were saved with the Zeiss LSM 5 Image software as .lsm raw data files. Post acquisition, Zeiss LSM Image Browser and ZEN-LE software were used to perform image adjustments (in single or multiple channels): brightness and contrast, color assignment, resizing, scaling, cropping, 3-D projections, orthographic projections and image output as compressed .jpeg files. Alternatively, z-stacks were exported as uncompressed .tiff series that were then processed with Daime software (Daims *et al*, 2006) for higher quality three dimensional volume-rendering with free rotation along the three Cartesian axes. The volume projections were exported as compressed .jpeg files.

50

CHAPTER 3. RESULTS AND DISCUSSION

3.1. Imaging on batch cultures of *C. thermocellum*

Initial attempts to characterize surface phenomena in *C. thermocellum* cultures during microbial cellulose utilization were made by microscopy investigations on batch grown cultures. The clear association with cellulose crystals was visible from the inspection of the culture vials (Figure 3.1). Growth around the cellulosic source which deposits at the bottom of the media container was primarily indicated by the presence of the yellow affinity substance. Growth in suspension (e.g. turbidity, flocs) was not visible in the bulk liquid, indicating that bacterial growth is mostly associated with attachment to the solid substrate.
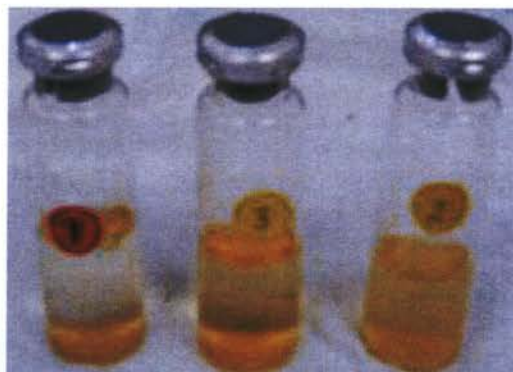
Figure 3.1 Image of typical *C. thermocellum* batch cultures showing growth associated with Avicel crystals deposited at the bottom of the serum vial (label 1); and resuspension after agitation (label 2 and 3).

Thus to investigate the potential of biofilm-like structure formation, samples were analyzed under epifluorescence microscopy. *C. thermocellum* was found to establish extensive biofilms on the surface of its solid cellulosic carbon source. Samples collected after 24 hour incubation were characterized by an abundance of terminal endospores, end-on attached at the non-sporulated side (Figure 3.2).
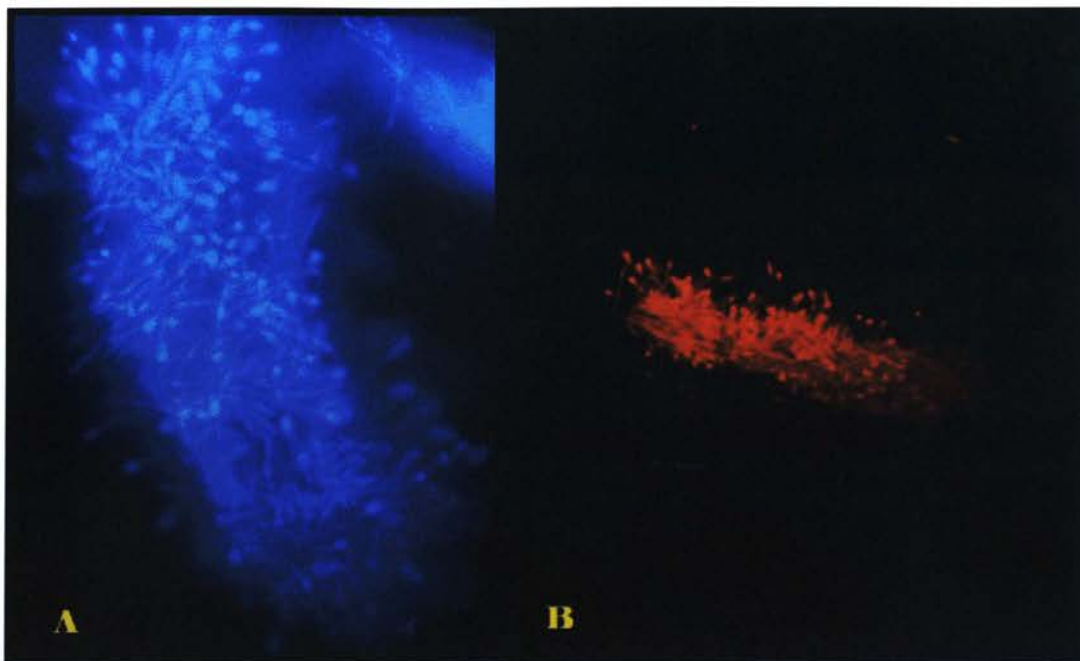
Figure 3.2 Epifluorescence micrographs of *Clostridium thermocellum* cells attached to Avicel crystals. A 24 hour old batch culture dominated by terminal endospore cells, end-on attached at the non-sporulating side. Staining with DAPi (A) and Ethidium Bromide (B); objective 63x1.4 oil immersion
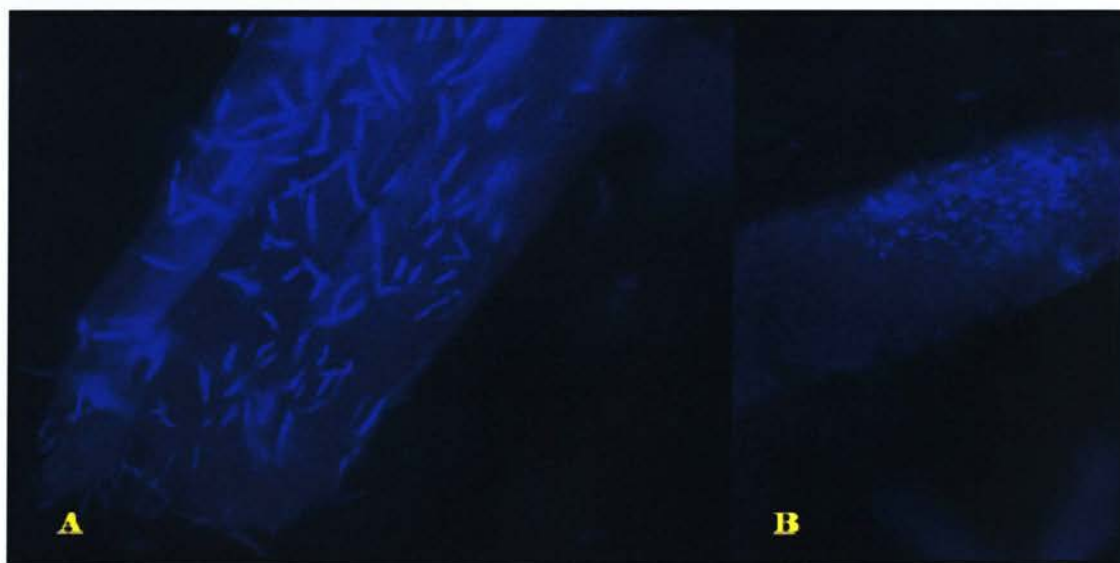
Figure 3.3 Epifluorescence micrographs of *Clostridium thermocellum* biofilms on Avicel crystals (in 48 hour old batch cultures). Cells attached to the substratum in a single layer, loosly (A) or tightly (B) packed. Staining with DAPI; objective 63x1.4 oil immersion.

Samples collected after 48 hours of growth were characterized by a majority of non-sporulated cells, with a predominant sideway orientation towards the solid substrate. Biofilms appeared to have a monolayer of cells (Figure 3.3), suggesting a close proximity of each individual cell to the solid substratum.

This procedure involved forcing the Avicel crystals twice through a needle with resulting increase in pressure flow. This suggested relatively strong cell-substrate attachment. Theoretically, each cellulose crystal can host an independent biofilm thus introducing the concept of a "community of biofilms" in pure culture growth; however, in the investigated batch cultures, biofilms in any particular sample appeared to be structurally similar, especially during the first 48 hours of incubation.

3.2. Imaging on continuous-flow cultures of *C. thermocellum*

The limitations of batch culture imaging (e.g. mechanical stress on adherent cells during sample preparations) were overcome with the continuous-flow culture observations of the fully hydrated, anaerobic biofilms. Sample preparation and handling ensured the bacteria were not exposed to additional stress factors. The 63x1.2 water immersion objective with a 0.24mm working distance dictated the range at which the solid cellulose could be imaged inside the flow chamber, directly through the glass cover slip. As introduced above, the concept of a community of biofilms within a single sample can also be applied to continuous-flow cultures where attachment was localized as populations of cells along cellulose fibers. However, growth in flow chambers was recorded to initiate around the inoculation site, and then to progressively spread and colonize the available adjacent cellulosic surface areas with concomitant depletion of

the solid substratum, which was their only cellulose source (Figure 3.4). Within the flow chamber, biofilms were observed at various degrees of cellulose colonization, from scattered cell groups to regions with very high cell densities, covering the entire surface areas of the fibers (Figure 3.5). Occasionally, attachment to inert glass surfaces was recorded in late growth stages primarily around substrate depletion zones. The attachment was characterized as monolayered cell clusters and it appears that this growth occurred primarily where cellulose was originally in contact with the glass (see panel D in Figure 3.5).
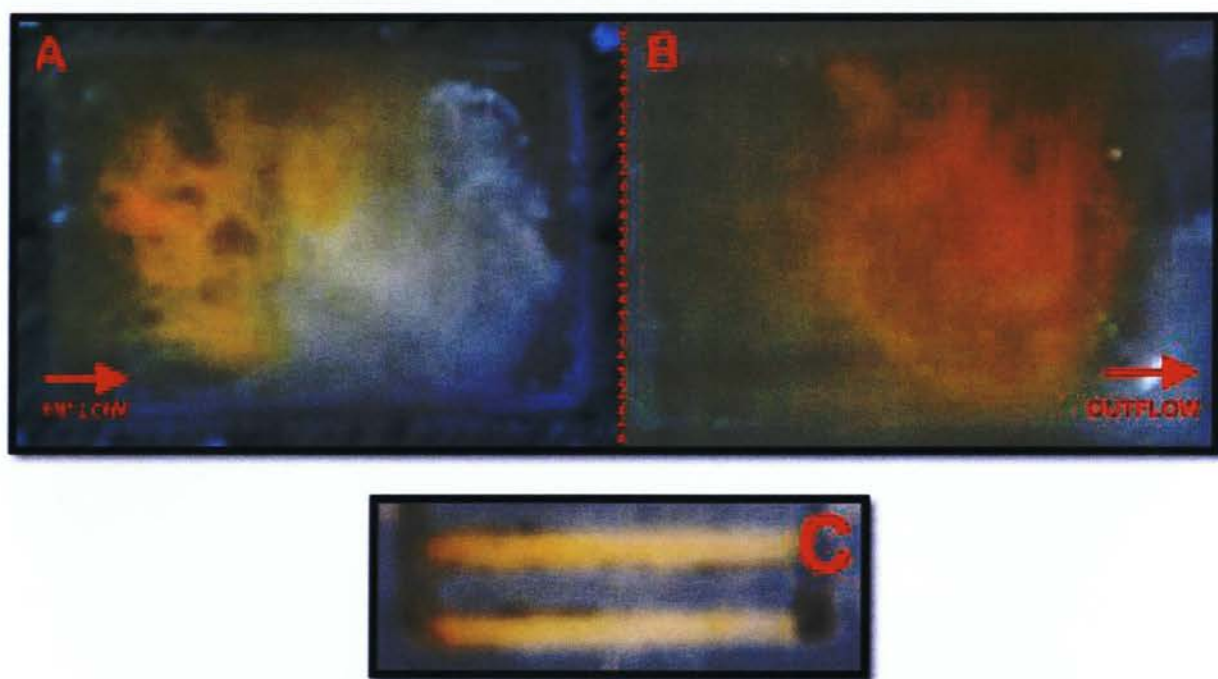
Figure 3.4 Typical *C. thermocellum* continuous-flow culture growth within flow cells showing the initial growth pattern around the inoculation site (A) with subsequent spreading to un-colonized regions and the depletion of its only cellulosic carbon source which serves as the attachment substratum (B); multi-channel flow chambers (C) showed the spreading (left to right in this case).
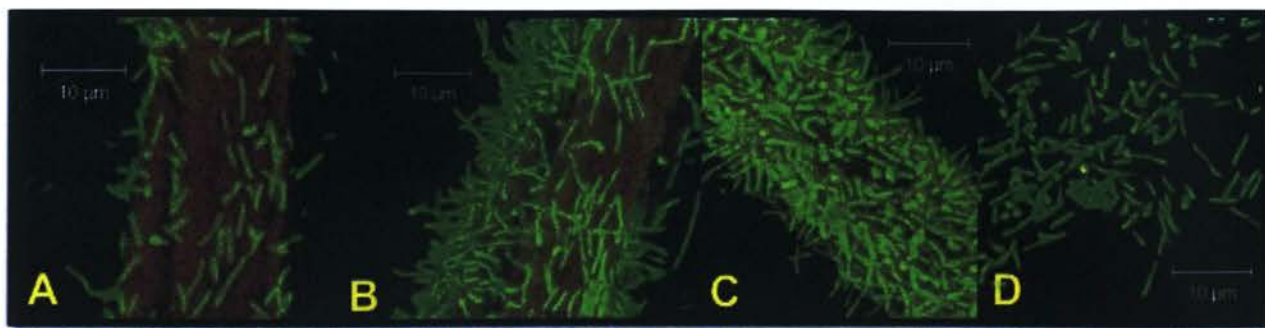
Figure 3.5 Confocal laser scanning micrographs of *Clostridium thermocellum* biofilms growing on solid cellulosic substratum. The colonization of the cellulose fibers develops with increasing cell density and subsequent spreading to unpopulated regions (A, B, C). Attachment to abiotic surfaces was recorded when the solid cellulosic support had been considerably depleted (D). Cells stained with Syto 9 (green); cellulose with WGA-TRITC (red).

Typical *C. thermocellum* biofilm morphology (Figure 3.6) was characterized by accumulations of terminal endospore and rod-shaped vegetative cells to the interface of solid cellulosic substratum, forming a single layer of cells with various degrees of density and with multiple cell orientations with regards to the attachment surface. Cells with terminal endospores had an invariable end-on attachment, and vegetative cells during division (see red circles, Figure 3.6) appeared to have a parallel orientation to the substrate. Cells divided along their longitudinal axis while attached, thus forming the typical long chains of cells described in previous work, which were also encountered in the flow cell effluent. Each individual cell appeared to be in close proximity to the cellulosic interface as proven by the orthographic projections along the xz and yz planes (Figure 3.7); there was thus little evidence for multi-layered biofilms.

Figure 3.6 CLSM micrograph of *C. themocellum* cells colonizing a cellulose substrate (fiber); showing spores (arrows) with distinct end-on attachment at the non-sporulating side; cells (yellow) stained with Syto9, cellulose (white) with WGA-TRITC; objective 63x1.2 water immersion. The red circles indicate dividing cells with parallel orientation to the attachment interface.
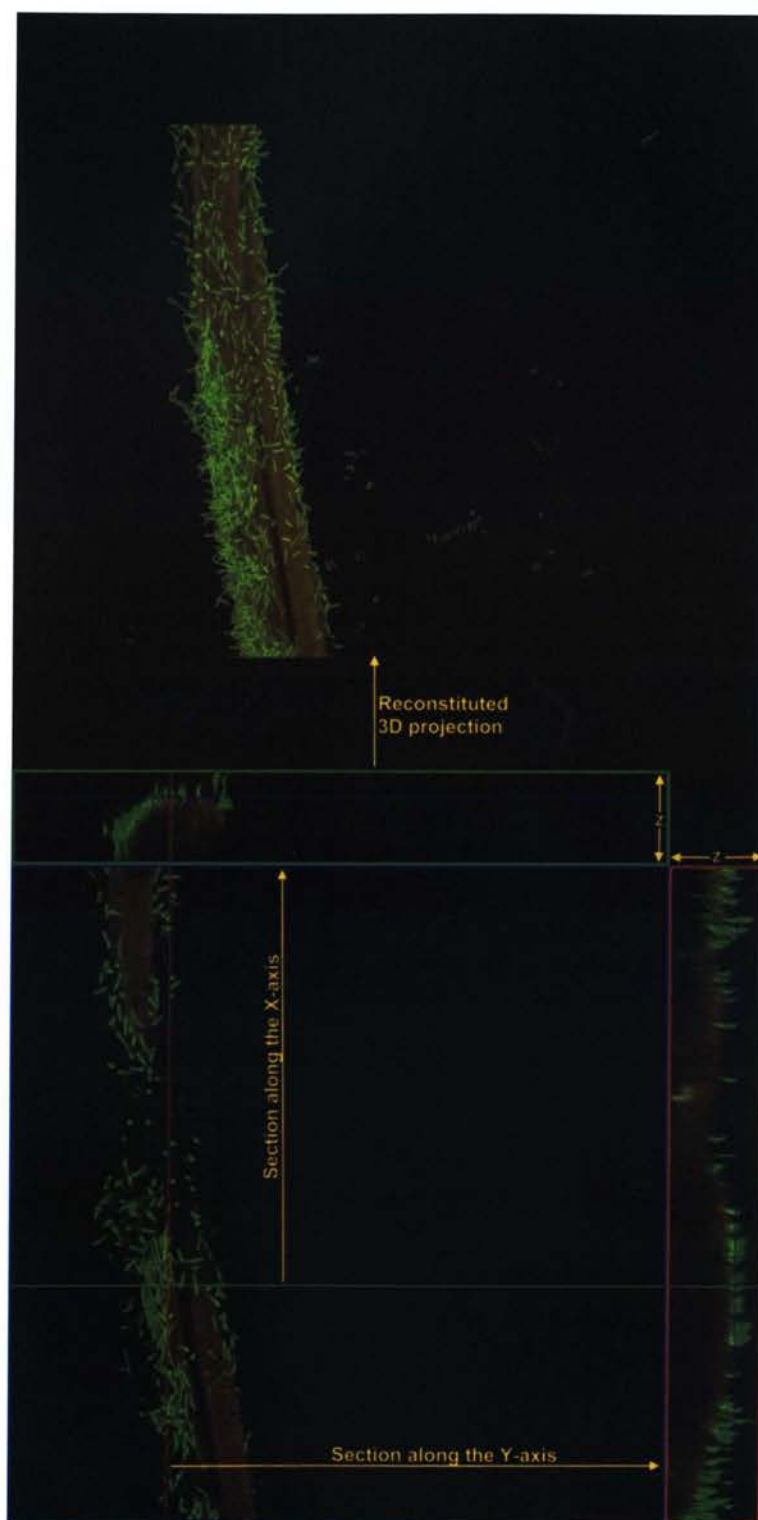
Figure 3.7 CLSM micrograph of *C. thermocellum* biofilm developing on a cellulose fiber seen from a top-down view of a three dimensional projection (top); sectioning through the projection along the X, Y axes in the Z plane (bottom) revealed the distance between cells and substrate which was recorded to be lower than the 0.44 μm z-scaling limit of the scanning microscope. Cells stained with Syto9 (green) and the cellulose with WGA-TRITC (red).

The minimum scaling capability along the z-axis was 0.44µm; therefore it can be stated with confidence that this is the maximum distance between the cell and substrate.

Cultures stained with high specificity conjugated lectins used in cocktail mixtures (covering the majority of known primary sugar specificity groups) or used individually failed to reveal a typical biofilm matrix of extracellular polymeric substance. The lectins adsorbed into the cellulosic fibers but did not bind or were not retained in a potential extracellular environment. At best, tetramethylrhodamine isothiocyanate (TRITC) conjugated Concanavalin A was recorded to bind cells (Figure 3.8) which pointed to the existence of a cell glycocalyx rather than an extensive EPS matrix.
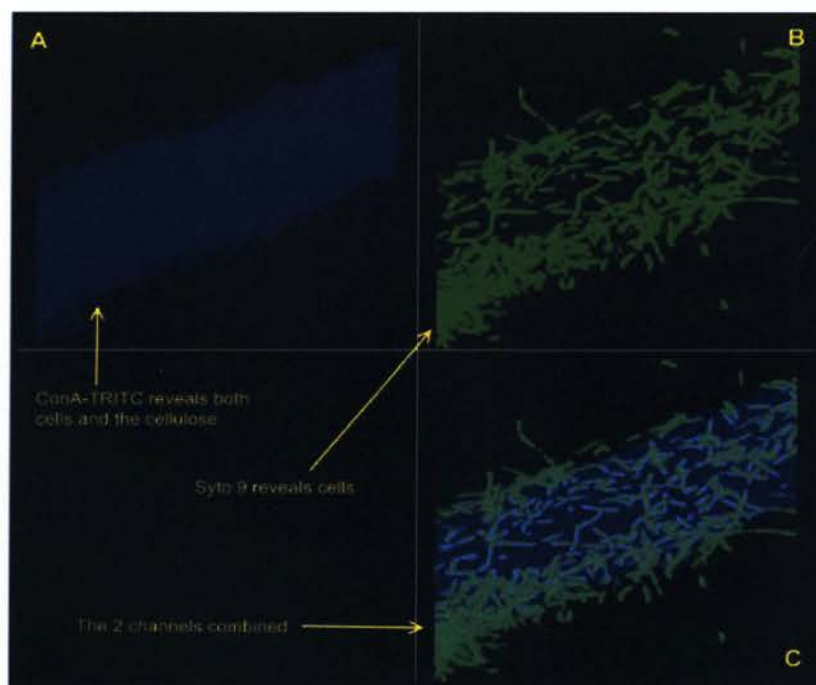
Figure 3.8 CLSM micrograph of *C. thermocellum* biofilms on cellulosic solid material. Cells are targeted with a general nucleic acid stain Syto 9 (panel B); a conjugated lectin Concanavalin A-TRITC with primary affinity for α-monnosyl and α-glucosyl residues binds both the cellulose and the cells indicating a potential EPS capsule (glycocalyx) individually surrounding each bacterial cell; the interpolation of these two channels is shown in panel C.

Biofilm model. The results from these microscopy investigations enabled the description of a proposed biofilm model for *Clostridium thermocellum* (Figure 3.10). This model should provide a foundation for further experiments aimed at delineating cell-substrate interaction by this important model bacterium, and should be expanded and modified in the event of new findings. The proposed model described initial cellular attachment through yet undefined mechanisms, potentially cellulosome-mediated, and the colonization of cellulosic substrates in a single layer of cells. Subsequent cellular division at the solid interface and sprawling with increasing density resulted in total surface area coverage, where vegetative cells adopted multiple orientations to the substratum and terminal endospores were invariably end-on attached. A typical biofilm matrix was absent and cell yield occurred at any stage after attachment.
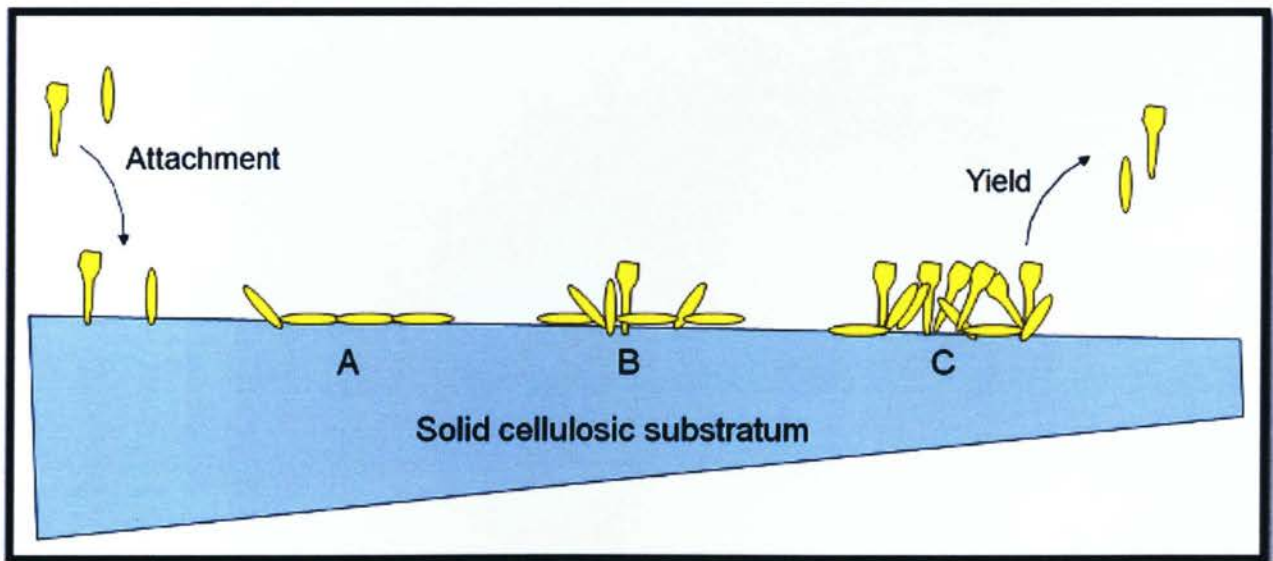
Figure 3.9 Proposed biofilm model for *C. thermocellum* showing initial attachment, colonization in monolayers of cells (A) with multiple cell orientations (B) and increasing density and distribution but with invariably end-on attached spores (C); cell yield can occur at any point after attachment.

3.3. Control experiment. Non-cellulolytic *S. cerevisiae* in simultaneous saccharification and fermentation (SSF)

Control experiments were carried out with non-cellulolytic organisms grown in continuous-flow mode on solid cellulosic substrate as the only carbon source with added cellulases to simulate the process known as simultaneous saccharification and fermentation (SSF). *S. cereviasiae* was found to grown at distance from the cellulose source (Figure 3.11), with cells attached to the glass cover slip or free floating between the cotton fibers.

Figure 3.10 CLSM micrograph of *S. cerevisiae* vin13 grown in the presence of celullose and free cellulolytic enzymes; cells are shown attached to the glass surface or free floating between cotton fibers; cells (yellow) stained with ethidium bromide, Cotton fiber (blue) adsorbed the stain too which rendered it detectable under excitation. Artificial coloring.

3.4. Imaging strategy and high quality volume rendering

Table 3.1 presents a summary of the range of fluorophores used in this study on batch and continuous-flow *C. thermocellum* cultures, including comments based on their suitability.

Table 3.1 Targeted staining of cellular and extracellular components in *C. thermocellum* biofilms

Group	Fluorophore	Primary target	Effect on cell	Experimental observations
Nucleic Acid Stains	SYTO 9	DNA / RNA		Excellent binding and strong fluorescence
	Acridine Orange	dsDNA / ssDNA / ssRNA		Non-specific binding
	DAPI	dsDNA	Invasive	Suitable for epifluorescence microscopy
	Ethidium bromide	dsDNA		Suitable for emission fluorescence above 600 nm
Lipid Stains	Nile Red	Intracellular lipids & hydrophobic domains of proteins	Non-toxic	Low emission fluorescence
	Lipophilic styryl compounds FM1-43 and FM4-64	Outer leaflet of cell membranes		Suitable for non-toxic, long term biofilm cell staining
Carbohydrate stains	Fluorophore-conjugated lectins	Primary sugars: Glucose, Mannose, Galactose, Fucose, N-Acetyl Galactosamine, N-Acetyl Glucosamine	Non-toxic	Limited use due to high binding specificity; typically used to target EPS/glycocalyx components.

This information should be applicable to future studies of cellulolytic biofilms. SYTO9 and DAPI were found to be the nucleic acid stains of choice in confocal laser scanning microscopy and fluorescence microscopy respectively. Due to its covalent binding and electrostatic interaction with nucleic acids Acridine orange was found to be

not suitable for *in-situ* biofilm staining, while Ethidium bromide was useful in multi-dye preparations where a cellular fluorescence signal above 600nm was desired. Non-toxic lipid stains were found useful in long term biofilm staining, with potential use in time-lapse microscopy, and the lipophilic styryl compounds FM1-43 and FM4-64 were found to have greater emission fluorescence with good spectrum coverage as opposed to the much cheaper but weakly fluorescent Nile Red. Conjugated lectins had limited use in *C. thermocellum* biofilm staining, possibly due to their high binding specificity. Their utility therefore needs further investigation.
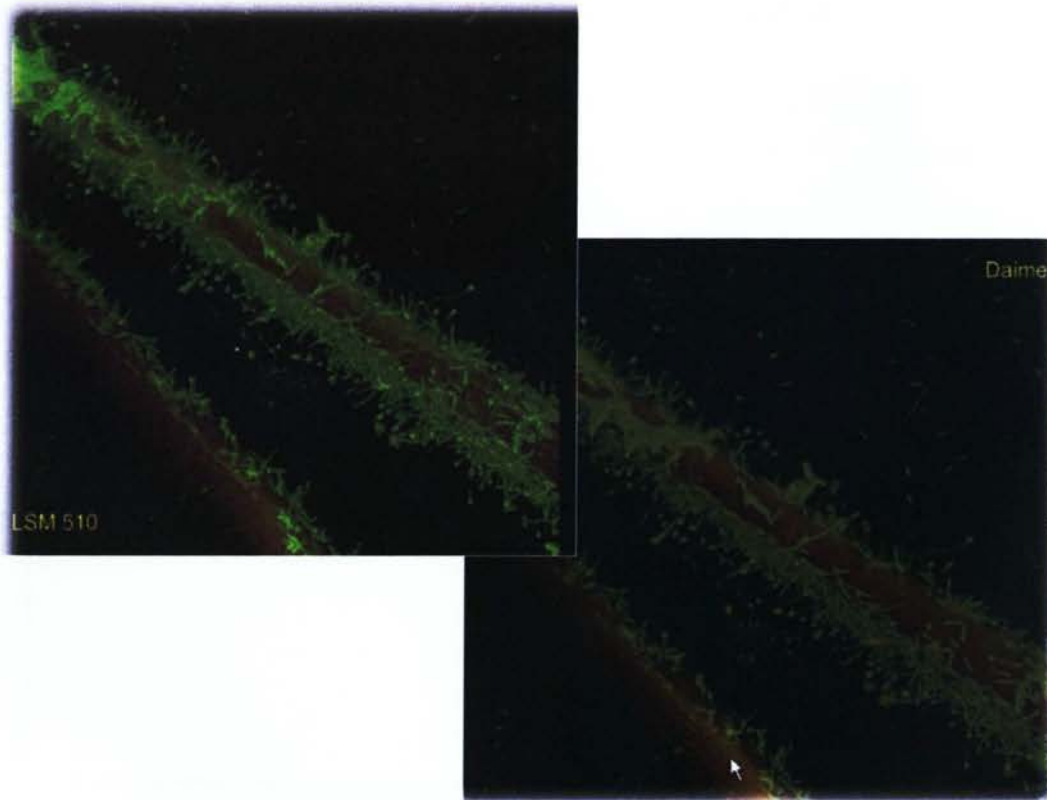
Figure 3.11 Post acquisition three-dimensional volume rendering of CLSM image stacks using the LSM 510 software (left) and the Daime software (right).

Optical xy sections along the z-axis were reconstituted as three dimensional projections of the scanned sample volumes. The high quality volume rendering function

of the Daime software was found to reduce random noise and increase contrast between the signal in different channels and the background (Figure 3.12). It also allowed free rotation of the projected volume along all three Cartesian axes (see Figure 3.13).
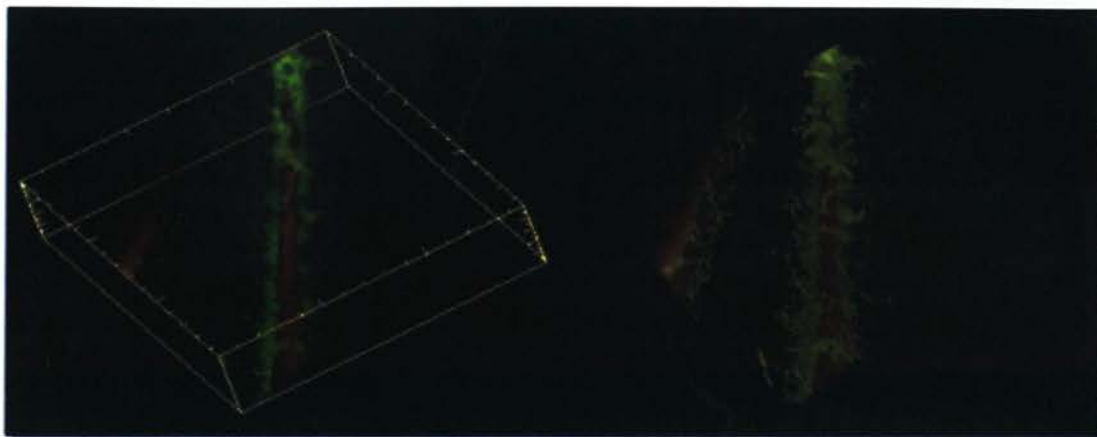
Figure 3.12 Quick 3D and High quality volume rendering of CLSM image stacks using the Daime software with free rotation along the X, Y and Z axes.

3.5. Analyses of flow cell effluent as indicator of *C. thermocellum* biofilm activity

3.5.1. Upstream inoculation flow cells

The inoculum from stock culture was introduced at the influent side of the flow chamber and continuous-flow maintained for 125 hours. Visual observations revealed a rapid biofilm spread with aggressive cellulose consumption. Samples collected at time zero before inoculation, were used as base line measurements.

Carbon dioxide readings were used as an indirect qualitative measure of the metabolic activity of the attached cells and the planktonic population at any given time. In relative percentage values, CO_2 readings increased to 65.45% at 47 hours after inoculation and then in smaller increments to its maximum value at 123 hours of growth (Figure 3.13), suggesting a continuous increase in activity with biofilm spreading and cellulose consumption.

The total carbohydrate balance did not account for cells or solid cellulosic fragments larger than 0.22 µm (due to sample filtration prior to analysis). Therefore it was an indirect measure of unused carbohydrate from the influent medium (originating from yeast extract, which is represented by the baseline value at time 0) and carbohydrate release through the hydrolysis of solid cellulose in the flow chamber.

Table 3.2 Carbon dioxide, total carbohydrate (<0.22 µm) and total cell counts in the effluent

Time (hours)	CO_2 readings* (ppm)	CO_2 readings* $(x10^{-9} mol/mL)$	Total Carbohydrate $(\mu g/mL)$	Total Cell Count $(x10^5 cells/mL)$
0	0.0	0.0	104.64	-
26	8.0	46.2	92.69	19.45
47	25.0	144.3	108.37	46.34
71	31.0	178.9	113.08	35.94
99	33.5	193.4	100.23	30.35
123	38.2	220.5	91.86	66.29

* Note: Carbon Dioxide units are: ppm (moles $CO_2/10^6$ moles total gas) and mol/mL (moles CO_2 / mL effluent liquid). Values shown include baseline subtraction.
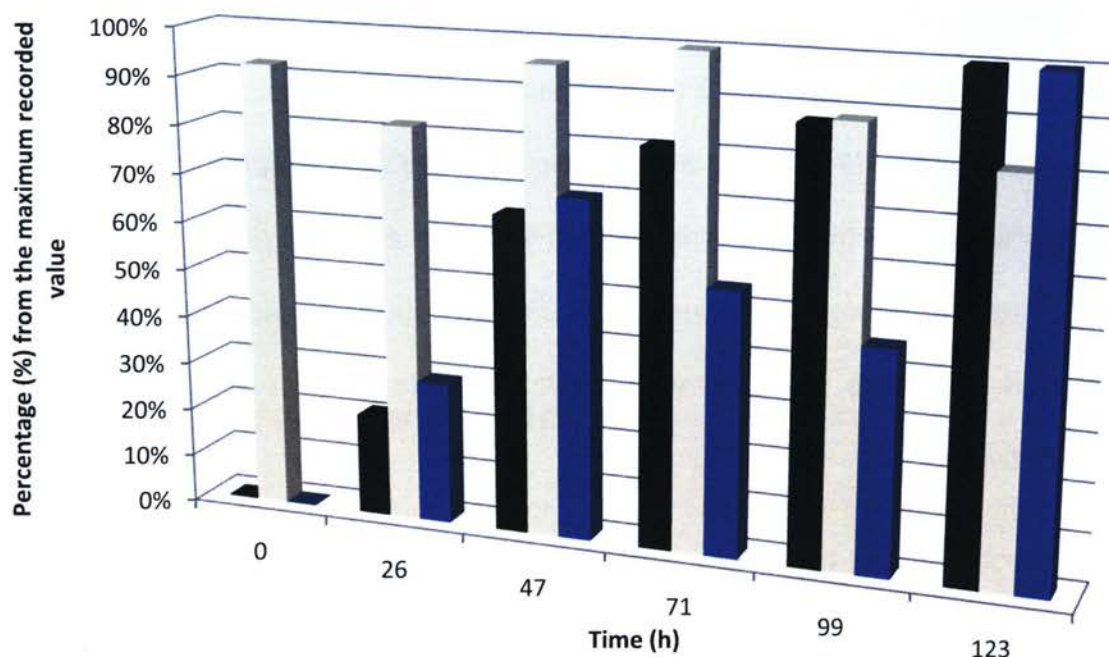
Figure 3.13 Relative values (percentage of maximum recorded values of the entire experiment) of the data in Table 3.2 showing increases in CO2 concentrations while the total carbohydrate (<0.22 μm fraction) remained relatively unchanged.

(■) Carbon dioxide; (☐) Total carbohydrate content; (■) Total cell counts

The Phenol-Sulfuric acid assay measures the concentration of simple sugars and their polymers (only pentoses, hexoses and heptoses; and no amino-sugars) and showed a minor variation from the baseline values over five days, suggesting a limited use of yeast extract carbon and an insignificant carbohydrate loss due to solid cellulose microbial hydrolysis. Solid cellulose used in the 4mL flow chamber was weighed to approximately 400mg (or 4×10^5μg), thus theoretically, the immobilized cellulose is in the 10^5 μg / mL flow chamber volume ratio.

Because the flow cell dilution rate greatly exceeded the maximum specific growth rate of *C. thermocellum*, the total cell counts can be expected to represent mostly detached cells eluted with the media from the biofilm chamber at any given time. The

method employed does not distinguish between live and dead cells, although with the short retention time (24 min.) it can be expected that most cells are alive. Direct microscopy measurements revealed a sharp increase in cell numbers at 47 hours (day two) and 123 hours (day five) after inoculation, reported as relative percentage values (against the highest recorded number) to 69.9% and 100.0% respectively, while day one, three and four were recorded with lower concentrations at 29.3%, 54.2% and 45.8%, respectively.

The direct counting technique allowed the classification of effluent cells in three distinct groups: normal vegetative cells, replicating cells or cells duplets that appeared to have undergone division (they were closely joined at one end, and were not confound with fragments from cell chains) and cell with terminal endospores.

Figure 3.14 Relative percentage values of cell types counted in *C. thermocellum* continuous-flow culture over five days of growth

(█) Normal cells; ( ) Replicating cells; (█) Sporulated cells

Reported as percentage values of the total cell counts per measurement (Figure 3.14), it was noted that the fraction of replicating cells gradually decreases from day one to day five from 28.0% to 8.8% respectively. The sporulated cell fraction increases from approximately 3% in day one to a maximum ratio on day five of 10% (Appendix table A1.3).

3.5.2. Downstream inoculation

A continuous-flow culture was grown for 145 hours (or approximately 6 days) where the inoculum from stock culture was introduced at the effluent side of the flow chamber. Visual observations recorded a slow, stunted, biofilm spreading with nearly half the flow chamber cellulose not showing the presence of the typical yellow affinity substance. Cell numbers in the effluent were about 50% (Table 3.3) of that in the case where inoculation was done upstream (Table 3.2).

Table 3.3 Carbon dioxide, total carbohydrate (<0.22 µm) and total cell counts in the effluent

Time (hours)	CO_2 readings* (ppm)	CO_2 readings* (10^{-9} mol/mL)	Total Carbohydrate (µg/mL)	Total Cell Count ($x10^5$ cells/mL)
0	0.0	0.0	96.90	-
24	4.9	28.3	98.69	20.37
47	6.4	36.9	88.92	8.17
70	8.6	49.6	90.92	10.13
95	10.4	60.0	91.47	11.84
124	13.6	78.5	87.98	23.52
145	15.4	88.9	80.94	30.26

* Note: Carbon Dioxide units are: ppm (moles $CO_2/10^6$ moles total gas) and mol/mL (moles CO_2 / mL effluent liquid). Values shown include baseline subtraction.

Carbon dioxide readings showed a steady increase in overall activity, expressed in relative percentage values as a midpoint 55.8% CO_2 at 70 hours and a maximum 100.0% at 145 hours (Figure 3.15)
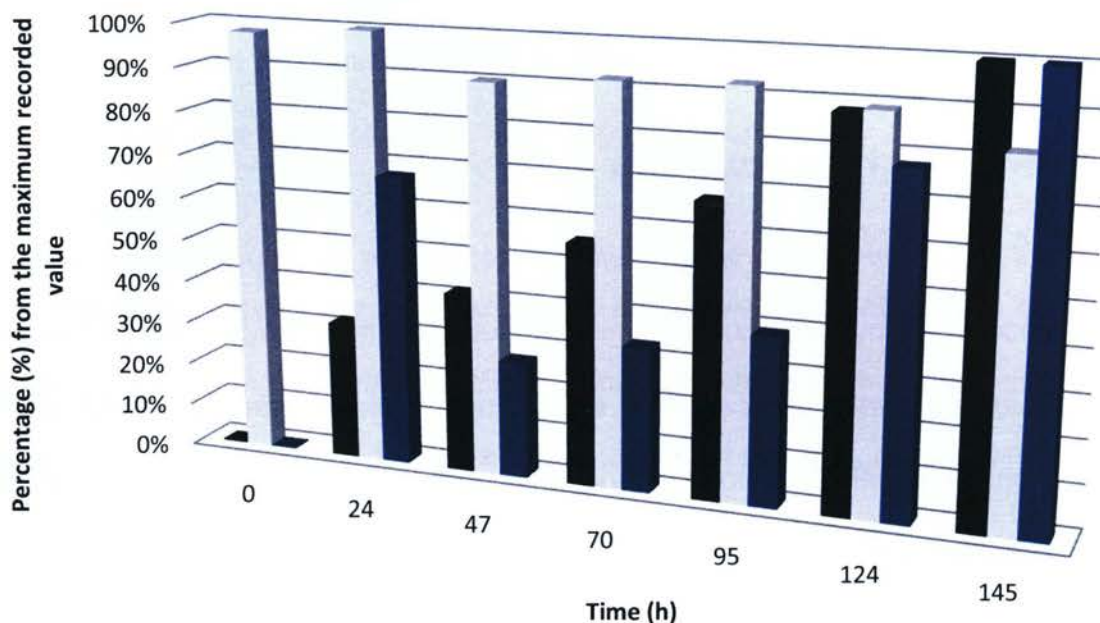
Figure 3.15 Relative values (percentage of maximum value during the entire experiment) of the data in Table 3.3.

(■) Carbon dioxide; ( ) Total carbohydrate content; (■) Total cell counts

Total carbohydrate measurements showed little variation from the baseline value of 96.9 ppm (see Table 3.3) with a slight increase at 24 hours and then a range of concentrations lower than the starting measured total carbohydrate. A minimum was recorded at 145 hours representing a 16.5% decrease from the baseline concentration.

Total suspended cell counts, expressed in relative percentage values with respect to the maximum recorded at 145 hours (Figure 3.15), showed a 63.3% peak value at 24 hours, a sharp decrease to 27.0% at 47 hours, a slow upward trend in the

following two days towards a 77.7% at 124 hours and the maximum concentration of eluted cells on day six.

Sporulated cells reached a maximum of 14.7% of the sample total cell number after 24 hours of growth, quickly decreasing to approximately 1% towards 124 hours and six (Figure 3.16). The replicating cells fraction remained constant at approximately 7% at 24 hours through 95 hours after inoculation and nearly doubled in number at 124 and 145 hours to circa 12%.

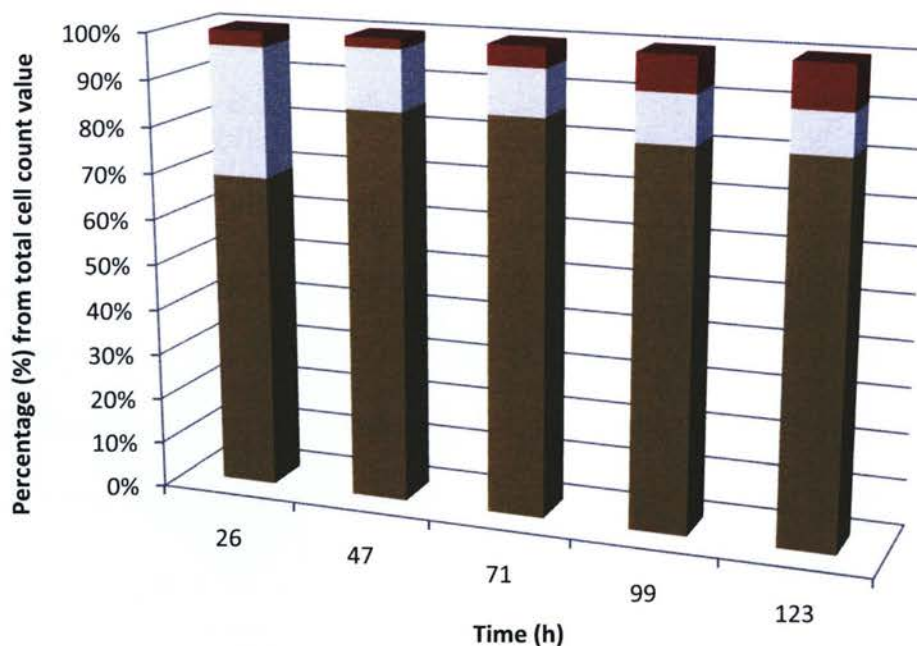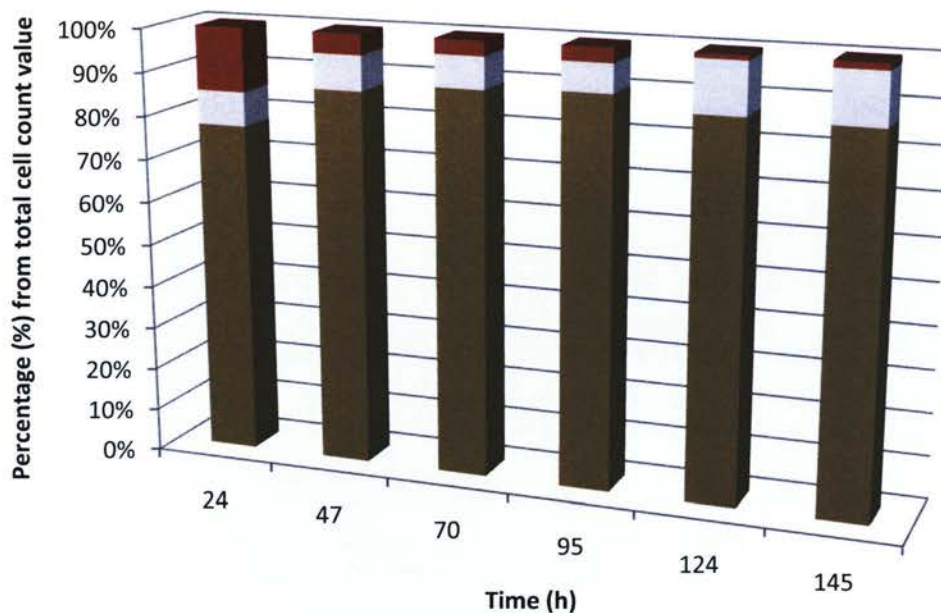**Figure 3.16 Relative percentage values of cell types counted in *C. thermocellum* continuous-flow culture over six days.**

( ) Normal cells; ( ) Replicating cells; ( ) Sporulated cells

3.6. **Discussion**

Early observations on batch cultures of *Clostridium thermocellum* showed cellular growth in close association with crystalline cellulose as indicated by the presence of the yellow affinity substance around the gravity deposited Avicel crystals. Direct epifluorescence microscopy observations revealed biofilm formation in monolayers of cells with varying degrees of surface area colonization densities. Spores were observed early in the batch incubation period, with some Avicel fragments being completely covered in end-on attached terminal endospores 24 hours after inoculation. The sporulation event has been described to occur due to stress factor such as pH drop below 6.4 or due to prolonged exposure to temperatures below 45^0C (Freier *et al*, 1988), which is reflective of stock culture conditions of either 60^oC vials where continued growth and end-product concentration lowers the pH below the proposed threshold or of 4^oC stored vials where spore cell prevalence has been confirmed with direct microscopic observations (not shown in Results). The presence of a high number of attached spores 24 hours into the incubation period of fresh cultures is indicative of: i) the direct involvement of sporulated cells in the adhesion to solid cellulosic substratum, ii) the involvement of spores in early mechanisms of cell translocation events to un-colonized cellulosic regions or iii) the existence of other regulatory mechanisms for sporulation initiation, independent of pH and temperature stress factors. The persistence of adherent cells despite the mechanical stress of batch cultures sample preparation is indicative of strong adhesion mechanisms of each individual cell to the substratum. The concept of a community of biofilms, where each Avicel microcrystal hosts an independent biofilm, can be applied to batch culture growth mode; therefore

population behavior should be analyzed from the perspective of the sum behavior of independent biofilms and the total number of non-attached cells.

In continuous-flow growth mode, microscopic imaging was performed *in-situ* and in fully hydrated anaerobic conditions. A community of biofilms was observed where each cellulose fiber is colonized with varying degrees of cell density and distribution. Applying this conceptual model, each flow cell hosts independent biofilms in different stages of development. Confocal laser scanning and post-acquisition image analysis allowed the description of a proposed biofilm model. Following initial attachment, cells divide along the longitudinal axis increasing the biofilm cell density sideways but not upwards; biofilm maturation might be coupled with the continuous recruitment of cells from the planktonic mode. Adherent cells were always visualized in monolayers, having various orientations to the attachment substratum. This observation supports the idea that the cellulolytic organisms requires close proximity to the cellulosic source for efficient substrate utilization and that carbohydrate capture from the liquid bulk phase (or the leeching of hydrolytic products from enzymatic cellulolysis) is not the preferred mode of life. Cellulose colonization progresses from localized patched of adherent cells to the complete coverage of the entire surface area. Predominantly on highly populated cellulose fibers, spores were observed with and invariable end-on attachment at the non-sporulated side. These cells might be involved in the mechanism of biofilm translocation to uncolonized regions and the sporulation events could be regulated by surface localized conditions or by cell to cell interactions in the biofilm layer. Carbohydrate and protein targeted staining in continuous-flow biofilms failed to reveal a typical EPS matrix interconnecting the adherent cells. However, TRITC conjugated

Concanavalin-A, with primary sugar specificity for α-glucose and α-mannose did reveal cells in biofilms, which is an indication of potential glycocalyx secretion. Previous electron microscopy findings suggest the existence of protracted polycellulosome protuberance at the surface of the adherent cells, mediating the contact between cellulose and the microbe (Bayer and Lamed, 1986). We propose that a glycocalyx layer is also involved in the cell-substrate interaction, as evidenced by observations of microbe adherence to inert surfaces in regions where cellulose was believed to have been in contact with the inert interface. Attachment to inert material suggests the existence of secondary, non-specific, binding mechanisms mediated for example by the constituents of a glycocalyx. Orthographic projections along the xz and yz planes of colonized cellulose fibers scanned along the vertical axis with a scaling of 0.44µm between sequential images in the xy plane revealed no visible distance between the microbes and the interface confirming a cell-substrate gap no larger than the 0.44µm.

The role of spores in translocation mechanisms, cellular division and biofilm lateral sprawling along the liquid-cellulose interface with subsequent detachment events and substrate depletion can be further understood by the use of time-lapse microscopy, a feature not yet encountered in the study of thermophilic anaerobic organisms. The formation of monolayer biofilms of strongly adherent cellulolytic cells, emphasizing the intimate association with the carbon substrate, can be further investigated in microbial consortia biofilms, where targeted staining techniques have to be developed to enable the in-situ localization of cellulolytic microbes in the consortium structures, which have previously been reported to form multilayer biofilms (O'Sullivan et al, 2008b).

A qualitative approach to flow cell biofilms activity was carried out by effluent measurements on dissolved carbon dioxide evolution, total carbohydrate by the phenol-sulfuric acid reaction, and total cell counts by direct epifluorescence technique. Two experimental conditions were tested: i) first, the inoculum was introduced at the flow cell influent side (upstream) and medium flow was started after one hour, ii) secondly, the inoculum was introduced at the effluent side (downstream) of the flow chamber and the continuous-flow was initiated after one hour. Theoretically, the upstream culture benefits from medium flow for quick transport and colonization of the entire available flow chamber cellulose. The downstream culture would require to translocate against the flow current to colonize new cellulose regions. The theoretical difference in colonization spreading was visually confirmed at the end of the incubation periods by the presence of the yellow affinity substance on the entire cellulose surface in the upstream culture and only in half of the flow chamber in the downstream experiment. Biofilm activity measurements indicate a twofold higher concentration of eluted dissolved CO_2 (mol/mL) and an overall similar ratio in total detached cells (cells/mL) from the upstream inoculation setup. Total carbohydrates (<0.22μm fragments) captured in the eflfuent remained relatively unchanged from the media baseline values, and with similar concentrations in both experiments.

Carbon dioxide was measured with an Infrared gas analyzer as parts per million units from the total gas leaving the "CO_2 exchange reactor" (Figure 2.5) at 25mL/min. The conditions of temperature (T = 324.58 K), and pressure (p = 99.70 x 10^3 N/m²) are constant in the gas analyzer measuring unit, thus using the equation of state for ideal gases the total gas molar volume V/n = RT/p = 27.07 x 10^3 ml/mol (where gas constant

R = 8.314 Nm/molK) was calculated. With a constant gas flow of 25mL/min, the rate of total moles of gas measured was calculated to be 0.9237×10^{-3} moles/min. Factoring the ppm readings (moles CO_2 / 10^6 moles total gas), and the constant rate (0.16mL/min) at which effluent liquid is entering the "CO_2 exchange reactor", and assuming free CO_2 is being transferred from the liquid to the gaseous form, the concentration of CO_2 (moles/mL) escaping the flow chamber as dissolved molecules was calculated (Table 3.2 and 3.3). Theoretically, a portion of CO_2 production from cellulolytic metabolism (the Embden-Meyerhoff pathway) will remain dissolved in the liquid phase as the bicarbonate ion (HCO_3^-); however with constant flow conditions which ensure unchanged pH and temperatures along the system, the ratio of free CO_2 and HCO_3^- remains constant. Therefore, the CO_2 detection with a gas analyzer represents a valid qualitative estimation of cellulolytic activity and consequently of biofilm biomass, development and spreading. In both experimental conditions, a continuous increase in activity was recorded during the entire incubation periods and this was correlated to an increase in microbial biomass or in biofilm spreading to un-colonized regions. These observations are in line with previously reported correlations on cellulose solubilization as heavily dependent on the quantity of biomass in the system (O'Sullivan *et al*, 2008a). The use of this novel technique in thermophilic, anaerobic, continuous-flow reactors has potential utilization for quick and simple on-line monitorization of biofilm communities' activity and estimation of biomass accumulation under optimal, constant conditions.

The phenol-sulfuric acid assays had been employed to provide a reliable index for total carbohydrate, due to its relative simplicity and insensitivity to interferences (Gerhardt *et al*, 1994). The phenol reaction is sensitive for pentoses, hexoses and

heptoses and their derivatives and polymers (except amino sugars) and it is insensitive to trioses and tetroses. Samples collected in the effluent were analyzed in triplicate, and compared with a prepared glucose standard (Appendix 3). In both experimental conditions the baseline carbohydrate detected in the media was approximately 100μg/mL, and there was little variation in the measured carbohydrate concentration in the effluent during the entire incubation period. Predominantly, the eluted carbohydrate had slightly lower concentration values, with a maximum recorded decreases of 16% from the reference baseline. The starting solid cellulose immobilized inside the flow chambers was in the 10^5 μg range (400mg cellulose in an approx. 4 mL chamber volume) and potential products resulting from cellulolysis (cellodextrins) were expected to produce a significant detectable change in the effluent particularly towards later stages of culture growth. The lack of significantly higher carbohydrate concentrations in the eluted media is supporting the idea that *Clostridium thermocellum* is a "cellulose specialist" and its close association with the cellulosic carbon substrate and the formation of ternary cellulose-enzyme-microbe complexes provides added benefits for optimal hydrolytic products capture.

The use of fluorochromes for the direct enumeration of total bacteria has been increasingly the method of choice for the estimation of total cell numbers (viable and non-viable or non-culturable), with important applications in the detection and control of bacterial population densities in microbial ecology studies (Kepner and Pratt, 1994). This method was ideal for sample collection in a normal oxygen atmosphere to accurately yield the total numbers of cells detached from the flow chamber community of biofilms. Effluent samples were analyzed in duplicate and in each counted dilution, 30

randomized fields were captured where the numbers of cells were in the 20 to 200 range. The method produced accurate and reproducible results, with a maximum total count standard deviation recorded at 12.0% and a minimum 1.1% (Appendix 1). The distribution of cells over the filtration area was found to have a maximum of 23.0% and a minimum of 9.6% variation from one microscopic field to another, as indicated by the counted numbers of cells per field in 30 randomized image captures of each sample. Generally, variation in cell distribution per field seemed to increase in the lower range of the 20 to 200 acceptable interval of cells per captured image. In the upstream inoculation experiment, the concentration of detached cells is generally twofold higher than the total cell counts in the downstream inoculated flow cell, which correlated to the estimates on cellulolytic activity and biofilm spreading. However, in both cases, variations between ~24 hour intervals seems to indicate a random pattern, which is consistent with previous observations that solid substrate depletion is followed by a sharp release of cells into the bulk liquid phase (Gelhaye *et al*, 1992). Biofilms nearing substrate depletion in the flow chamber community are responsible for the sharp release of cells into the effluent and the observed total cell count patterns are the sum behavior of all the biofilm structures in their different developmental stages. Direct total cell counts have the potential use as reliable indicators of total biofilms response to stress factors (chemical, physical or biological). Direct counting also allowed the classification of eluted cells in three groups: normal cells, dividing cells and spores. In both experiments, normal cells are generally within the 80% to 90% range of the sample total cell count; however, the fractions of dividing cells and spores follow opposite evolution trends. In the upstream inoculated flow chamber, dividing cells shift from

28.0% at 24 hours to 8.8% at 123 hours, whereas spores increase from 3.3% to 10.0% respectively. Having the medium flow as a dispersion mediator, biofilm spreading is much quicker, allowing for a more rapid increase in cell numbers. As previously mentioned, sporulated cells have been associated with densely colonized cellulose fibers, therefore an increase in eluted spores towards later stages of incubation equates to the increasing prevalence of dense biofilms in the community. In the downstream inoculated chamber, dividing cell fractions slightly increased from 7.8% to 11.8% of the total cell counts during the six day incubation period, whereas spores rapidly decreased from 14.7% at 24 hours to 4.8% at 47 hours and then gradually to 1.5% towards the end of incubation. These results indicate a more localized biofilm agglomeration at inoculation site with slower spreading against the medium flow. The high fraction of spores at 24 hours into the incubation suggests dense localized biofilm formations and also indicates the potential role of these stress-response cells in population translocation events.

3.7. Concluding statements

Clostridium thermocellum, naturally cellulolytic, thermophilic, anaerobic gram positive bacterium, capable of complete cellulolysis and ethanol production is a potential candidate for organism development through native cellulolytic strategies (Lynd *et al*, 2005) in the consolidated bioprocessing (CBP) approach to large scale conversion of renewable biomass into biofuels and other secondary products. Understanding organism behavior and its association with cellulosic substratum and optimizing new

investigation tools are important aspects in the advancement of biomass conversion process development. To achieve this goal, continuous-flow mini reactors were designed to enable the *in-situ* high resolution imaging of microbial biofilms. Additionally, a set of assays were applied on the effluent of upstream and downstream inoculated flow cells, over five and six day incubation periods, to monitor continuous-flow culture activity and dynamics. *C. thermocellum* was found to form strongly adherent monolayer biofilms, with a cell-substrate distance under $0.44\mu m$. Results suggest an individual cell glycocalyx involved in strengthening adhesion to interfaces while targeted probing failed to reveal the presence of an EPS matrix. Sporulated cells are invariably end-on attached at the non-sporulated side, more prevalent in regions with high cell density, and are believed to be involved in biofilm translocation to uncolonized regions. The concept of a pure culture "community of biofilms" was introduced to understand the behavior of adherent cells where the only cellulosic carbon source (in the form of fibers) served as the attachment interface as well. Total carbohydrate measurement in the eluted samples, did not reveal a significant loss of cellodextrins, supporting the idea of enhanced substrate capture by the highly specialized adherent organisms. Carbon dioxide gas "exchange reactors" were successfully employed to qualitatively monitor the cellulolytic culture activity and direct enumeration of total detached cells showed significant variation in cell type fractions dependent on culturing conditions as well as supporting the idea of sharp release of cells into the bulk liquid medium with the depletion of solid substrates.

REFERENCES

1. Bais, H.P., Fall, R., and Vivanco, J.M. 2004. Biocontrol of Bacillus subtilis against Infection of Arabidopsis Roots by Pseudomonas syringae Is Facilitated by Biofilm Formation and Surfactin Production. Plant Physiology **134**(1): 307-319.

2. Bayer, E.A., and Lamed, R. 1986. Ultrastructure of the cell surface cellulosome of clostridium thermocellum and its interaction with cellulose. Journal of Bacteriology **167**(3): 828-836.

3. Bayer, E.A., Setter, E., and Lamed, R. 1985. Organization and distribution of the cellulosome in Clostridium thermocellum. Journal of Bacteriology **163**(2): 552-559.

4. Bayer, E.A., Kenig, R., and Lamed, R. 1983. Adherence of Clostridium thermocellum to cellulose. Journal of Bacteriology **156**(2): 818-827.

5. Bayer, E.A., Shimon, L.J.W., Shoham, Y., and Lamed, R. 1998. Cellulosomes - Structure and ultrastructure. Journal of Structural Biology **124**(2-3): 221-234.

6. Beech, I.B., Sunner, J.A., and Hiraoka, K. 2005. Microbe-surface interactions in biofouling and biocorrosion processes. International Microbiology **8**(3): 157-168.

7. Béguin, P., and Aubert, J.-. 1994. The biological degradation of cellulose. FEMS Microbiology Reviews **13**(1): 25-58.

8. Coetser, S.E., and Cloete, T.E. 2005. Biofouling and biocorrosion in industrial water systems. Critical Reviews in Microbiology **31**(4): 213-232.

9. Costerton, J.W. 1995. Overview of microbial biofilms. Journal of Industrial Microbiology **15**(3): 137-140.

10. Daims, H., Lücker, S., and Wagner, M. 2006. *daime*, a novel image analysis program for microbial ecology and biofilm research. Environmental Microbiology **8**(2): 200-213.

11. Davies, D.G., Parsek, M.R., Pearson, J.P., Iglewski, B.H., Costerton, J.W., and Greenberg, E.P. 1998. The involvement of cell-to-cell signals in the development of a bacterial biofilm. Science **280**(5361): 295-298.

12. Demain, A.L., Newcomb, M., and Wu, J.H.D. 2005. Cellulase, clostridia, and ethanol. Microbiology and Molecular Biology Reviews **69**(1): 124-154.

13. Dismukes, G.C., Carrieri, D., Bennette, N., Ananyev, G.M., and Posewitz, M.C. 2008. Aquatic phototrophs: efficient alternatives to land-based crops for biofuels. Current Opinion in Biotechnology **19**(3): 235-240.

14. Farrell, A.E., Plevin, R.J., Turner, B.T., Jones, A.D., O'Hare, M., and Kammen, D.M. 2006. Ethanol can contribute to energy and environmental goals. Science **311**(5760): 506-508.

15. Freier, D., Mothershed, C.P., and Wiegel, J. 1988. Characterization of Clostridium thermocellum JW20. Appl. Environ. Microbiol. **54**(1): 204-211.

16. Fronzes, R., Remaut, H., and Waksman, G. 2008. Architectures and biogenesis of non-flagellar protein appendages in Gram-negative bacteria. EMBO Journal **27**(17): 2271-2280.

17. Fukushima, R.S., Weimer, P.J., and Kunz, D.A. 2003. Use of photocatalytic reduction to hasten preparation of culture media for saccharolytic *Clostridium* species. Brazilian Journal of Microbiology **34**: 22-26.

18. Gaudet, G., and Gaillard, B. 1987. Vesicle formation and cellulose degradation in Bacteroides succinogenes cultures: Ultrastructural aspects. Archives of Microbiology **148**(2): 150-154.

19. Gelhaye, E., Petitdemange, H., and Gay, R. 1992. Characteristics of cellulose colonization by a mesophilic, cellulolytic Clostridium (strain C401). Research in Microbiology **143**(9): 891-895.

20. Gerhardt, P., Krieg, N.R., Murray, R.G.E., and Wood, W.A. (Editors). 1994. Methods for General and Molecular Bacteriology. The American Society for Microbiology, Washington, D.C.

21. Greene, N., Celik, F., Dale, B., and Jackson, M. 2004. Growing energy: How biofuels can help end America's oil dependence. Natural Resources Defense Council .

22. Gutiérrez-Lomelí, M., Torres-Guzmán, J.C., González-Hernández, G.A., Cira-Chávez, L.A., Pelayo-Ortiz, C., and Ramírez -Córdova, J.d.J. 2008. Overexpression of ADH1 and HXT1 genes in the yeast Saccharomyces cerevisiae improves the fermentative efficiency during tequila elaboration. Antonie van Leeuwenhoek, International Journal of General and Molecular Microbiology **93**(4): 363-371.

23. Hall-Stoodley, L., and Stoodley, P. 2005. Biofilm formation and dispersal and the transmission of human pathogens. Trends in Microbiology **13**(1): 7-10.

24. Hammerschlag, R. 2006. Ethanol's energy return on investment: A survey of the literature 1990 - Present. Environmental Science and Technology **40**(6): 1744-1750.

25. Hansen, M.C., Palmer Jr., R.J., and White, D.C. 2000. Flowcell culture of Porphyromonas gingivalis biofilms under anaerobic conditions. Journal of Microbiological Methods **40**(3): 233-239.

26. Henrichsen, J. 1972. Bacterial surface translocation: a survey and a classification. Bacteriological reviews **36**(4): 478-503.

27. Heydorn, A., Ersboll, B.K., Hentzer, M., Parsek, M.R., Givskov, M., and Molin, S. 2000a. Experimental reproducibility in flow-chamber biofilms. Microbiology **146**(10): 2409-2415.

28. Heydorn, A., Nielsen, A.T., Hentzer, M., Sternberg, C., Givskov, M., Ersboll, B.K., and Molin, S. 2000b. Quantification of biofilm structures by the novel computer program COMSTAT. Microbiology **146**(10): 2395-2407.

29. Hostalka, F., Moultrie, A., and Stutzenberger, F. 1992. Influence of carbon source on cell surface topology of Thermomonospora curvata. Journal of Bacteriology **174**(21): 7048-7052.

30. Hungate, R.E. 1969. A roll tube method for cultivation of strict anaerobes. Methods in Microbiology **3B**: 117-132.

31. Hungate, R.E. 1950. The anaerobic mesophilic cellulolytic bacteria. Bacteriological Reviews **14**(1): 1-49.

32. Jensen, P.D., Hardin, M.T., and Clarke, W.P. 2008. Measurement and quantification of sessile and planktonic microbial populations during the anaerobic digestion of cellulose. Water Science and Technology **57**(4): 465-469.

33. Jones, L.R., Watson-Craik, I.A., and Senior, E. 1997. Image analysis for the study of the development of anaerobic biofilms on materials characteristic of landfilled refuse. Water Science and Technology **36**(6-7): 485-492.

34. Jordan, N., Boody, G., Broussard, W., Glover, J.D., Keeney, D., McCown, B.H., McIsaac, G., Muller, M., Murray, H., Neal, J., Pansing, C., Turner, R.E., Warner, K., and Wyse, D. 2007. Sustainable development of the agricultural bio-economy. Science **316**(5831): 1570-1571.

35. Kepner Jr., R.L., and Pratt, J.R. 1994. Use of fluorochromes for direct enumeration of total bacteria in environmental samples: Past and present. Microbiological Reviews **58**(4): 603-615.

36. Kim, T.-., Young, B.M., and Young, G.M. 2008. Effect of flagellar mutations on Yersinia enterocolitica biofilm formation. Applied and Environmental Microbiology **74**(17): 5466-5474.

37. Kobayashi, K. 2008. SlrR/SlrA controls the initiation of biofilm formation in Bacillus subtilis. Molecular Microbiology **69**(6): 1399-1410.

38. Kopečný, J., and Hodrová, B. 1997. The effect of yellow affinity substance on cellulases of Ruminococcus flavefaciens. Letters in Applied Microbiology **25**(3): 191-196.

39. Krzanowski, S., and Wałega, A. 2008. Effectiveness of organic substance removal in household conventional activated sludge and hybrid treatment plants. Environment Protection Engineering **34**(3): 5-12.

40. Kudo, H., Cheng, K.-., and Costerton, J.W. 1987. Electron microscopic study of the methylcellulose-mediated detachment of cellulolytic rumen bacteria from cellulose fibers. Canadian Journal of Microbiology **33**(3): 267-272.

41. Lamed, R., Naimark, J., Morgenstern, E., and Bayer, E.A. 1987. Specialized cell surface structures in cellulolytic bacteria. Journal of Bacteriology **169**(8): 3792-3800.

42. Larsen, P., Olesen, B.H., Nielsen, P.H., and Nielsen, J.L. 2008. Quantification of lipids and protein in thin biofilms by fluorescence staining. Biofouling **24**(4): 241-250.

43. Ljungdahl, L.G., Pettersson, B., Eriksson, K.E., and Wiegel, J. 1983. A yellow affinity substance involved in the cellulolytic system of Clostridium thermocellum. Current Microbiology **9**(4): 195-199.

44. Lu, Y., Zhang, Y.P., and Lynd, L.R. 2006. Enzyme-microbe synergy during cellulose hydrolysis by Clostridium thermocellum. Proceedings of the National Academy of Sciences **103**(44): 16165-16169.

45. Lynd, L.R., Weimer, P.J., Wolfaardt, G., and Zhang, Y.-.P. 2006. Cellulose hydrolysis by Clostridium thermocellum: A microbial perspective. *In* Cellulosome. *Edited by* I.A. Kataeva. Nova Science Publishers, Inc., Hauppauge, NY, U.S.A. pp. 95-117.

46. Lynd, L.R. 2008. Energy biotechnology. Current Opinion in Biotechnology **19**(3): 199-201.

47. Lynd, L.R. 2007. Thermophilic bacterium for biomass ethanol. Industrial Bioprocessing **29**(6): 4.

48. Lynd, L.R. 1996. Overview and evaluation of fuel ethanol from cellulosic biomass: Technology, economics, the environment, and policy. Annual Review of Energy and the Environment **21**(1): 403-465.

49. Lynd, L.R., Grethlein, H.E., and Wolkin, R.H. 1989. Fermentation of cellulosic substrates in batch and continuous culture by Clostridium thermocellum. Applied and Environmental Microbiology **55**(12): 3131-3139.

50. Lynd, L.R., Van Zyl, W.H., McBride, J.E., and Laser, M. 2005. Consolidated bioprocessing of cellulosic biomass: An update. Current Opinion in Biotechnology **16**(5): 577-583.

51. Lynd, L.R., Weimer, P.J., Van Zyl, W.H., and Pretorius, I.S. 2002. Microbial cellulose utilization: Fundamentals and biotechnology. Microbiology and Molecular Biology Reviews **66**(3): 506-577.

52. Lynd, L.R., Laser, M.S., Bransby, D., Dale, B.E., Davison, B., Hamilton, R., Himmel, M., Keller, M., McMillan, J.D., Sheehan, J., and Wyman, C.E. 2008. How biotech can transform biofuels. Nature Biotechnology **26**(2): 169-172.

53. Mai, V., and Wiegel, J. 2000. Advances in development of a genetic system for Thermoanaerobacterium spp.: Expression of genes encoding hydrolytic enzymes, development of a second shuttle vector, and integration of genes into the chromosome. Applied and Environmental Microbiology **66**(11): 4817-4821.

54. Massana, R., Gasol, J.M., Bjørnsen, P.K., Blackburn, N., Hagström, A., Hietanen, S., Hygum, B.H., Kuparinen, J., and Pedrós -Alió, C. 1997. Measurement of bacterial size via image analysis of epifluorescence preparations: Description of an inexpensive system and solutions to some of the most common problems. Scientia Marina **61**(3): 397-407.

55. McBee, R.H. 1954. The characteristics of *Clostridium thermocellum*. The Journal of Bacteriology **67**: 505-506.

56. McBee, R.H. 1950. The anaerobic thermophilic cellulolytic bacteria. Bacteriological Revievs **14**(1): 51-63.

57. Merod, R.T., Warren, J.E., McCaslin, H., and Wuertz, S. 2007. Toward automated analysis of biofilm architecture: Bias caused by extraneous confocal laser scanning microscopy images. Applied and Environmental Microbiology **73**(15): 4922-4930.

58. Miron, J., and Forsberg, C.W. 1999. Characterisation of cellulose-binding proteins that are involved in the adhesion mechanism of Fibrobacter intestinalis DR7. Applied Microbiology and Biotechnology **51**(4): 491-497.

59. Miron, J., Ben-Ghedalia, D., and Morrison, M. 2001. Invited review: Adhesion mechanisms of rumen cellulolytic bacteria. Journal of Dairy Science **84**(6): 1294-1309.

60. Morris, E.J., and Cole, O.J. 1987. Relationship between cellulolytic activity and adhesion to cellulose in Ruminococcus albus. Journal of General Microbiology **133**(4): 1023-1032.

61. Morrison, M., and Miron, J. 2000. Adhesion to cellulose by Ruminococcus albus: A combination of cellulosomes and Pil-proteins? FEMS Microbiology Letters **185**(2): 109-115.

62. Nejadnik, M.R., van der Mei, H.C., Norde, W., and Busscher, H.J. 2008. Bacterial adhesion and growth on a polymer brush-coating. Biomaterials **29**(30): 4117-4121.

63. Nikolaev, Y.A., and Plakunov, V.K. 2007. Biofilm-"city of microbes" or an analogue of multicellular organisms? Microbiology **76**(2): 125-138.

64. O'Sullivan, C., Burrell, P.C., Clarke, W.P., and Blackall, L.L. 2008a. The effect of biomass density on cellulose solubilisation rates. Bioresource Technology **99**(11): 4723-4731.

65. O'Sullivan, C., Burrell, P.C., Pasmore, M., Clarke, W.P., and Blackall, L.L. 2008b. Application of flowcell technology for monitoring biofilm development and cellulose degradation in leachate and rumen systems. Bioresource Technology **100**(1): 492-496.

66. O'Sullivan, C.A., Burrell, P.C., Clarke, W.P., and Blackall, L.L. 2005. Structure of a cellulose degrading bacterial community during anaerobic digestion. Biotechnology and Bioengineering **92**(7): 871-878.

67. O'Toole, G.A., and Kolter, R. 1998. Flagellar and twitching motility are necessary for Pseudomonas aeruginosa biofilm development. Molecular Microbiology **30**(2): 295-304.

68. Otto, K. 2008. Biophysical approaches to study the dynamic process of bacterial adhesion. Research in Microbiology **159**(6): 415-422.

69. Ozkan, M., Desai, S.G., Zhang, Y., Stevenson, D.M., Beane, J., White, E.A., Guerinot, M.L., and Lynd, L.R. 2001. Characterization of 13 newly isolated strains of anaerobic, cellulolytic, thermophilic bacteria. Journal of Industrial Microbiology and Biotechnology **27**(5): 275-280.

70. Palmer Jr., R.J. 1999. Microscopy Flowcells: Perfusion chambers for real time study of biofilms. Methods in Enzymology **310**: 160-166.

71. Prigent-Combaret, C., Vidal, O., Dorel, C., and Lejeune, P. 1999. Abiotic surface sensing and biofilm-dependent regulation of gene expression in Escherichia coli. Journal of Bacteriology **181**(19): 5993-6002.

72. Purevdorj, B., Costerton, J.W., and Stoodley, P. 2002. Influence of hydrodynamics and cell signaling on the structure and behavior of Pseudomonas aeruginosa biofilms. Applied and Environmental Microbiology **68**(9): 4457-4464.

73. Rau, U., Kuenz, A., Wray, V., Nimtz, M., Wrenger, J., and Cicek, H. 2008. Production and structural analysis of the polysaccharide secreted by Trametes (Coriolus) versicolor ATCC 200801. Applied Microbiology and Biotechnology : 1-11.

74. Schwarz, W.H. 2001. The cellulosome and cellulose degradation by anaerobic bacteria. Applied Microbiology and Biotechnology **56**(5-6): 634-649.

75. Simões, M., Cleto, S., Pereira, M.O., and Vieira, M.J. 2007. Influence of biofilm composition on the resistance to detachment. Water Science and Technology **55**(8-9): 473-480.

76. Stoodley, P., Sauer, K., Davies, D.G., and Costerton, J.W. 2002. Biofilms as complex differentiated communities. Annual Review of Microbiology **56**: 187-209.

77. Strobel, H.J. 1995. Growth of the thermophilic bacterium Clostridium thermocellum in continuous culture. Current Microbiology **31**(4): 210-214.

78. Syutsubo, K., Nagaya, Y., Sakai, S., and Miya, A. 2005. Behavior of cellulose-degrading bacteria in thermophilic anaerobic digestion process. Water Science and Technology **52**(1-2): 79-84.

79. Tolker-Nielsen, T., Brinch, U.C., Ragas, P.C., Andersen, J.B., Jacobsen, C.S., and Molin, S. 2000. Development and dynamics of Pseudomonas sp. biofilms. Journal of Bacteriology **182**(22): 6482-6489.

80. Tsoĭ, T.V., Chuvil'skaia, N.A., Atakishieva, I.I., Dzhavakhishvili, T.T., and Akimenko, V.K. 1987. Clostridium thermocellum--a new object of genetic studies. Molekuliarnaia genetika, mikrobiologiia i virusologiia (11): 18-23.

81. Tyurin, M.V., Desai, S.G., and Lynd, L.R. 2004. Electrotransformation of Clostridium thermocellum. Applied and Environmental Microbiology **70**(2): 883-890.

82. Van Zyl, W.H., Lynd, L.R., Den Haan, R., and McBride, J.E. 2007. Consolidated bioprocessing for bioethanol production using saccharomyces cerevisiae. Advances in Biochemical Engineering/Biotechnology **108**: 205-235.

83. Verstraeten, N., Braeken, K., Debkumari, B., Fauvart, M., Fransaer, J., Vermant, J., and Michiels, J. 2008. Living on a surface: swarming and biofilm formation. Trends in Microbiology **16**(10): 496-506.

84. Viljoen, J.A., Fred, E.B., and Peterson, W.H. 1926. The fermentation of cellulose by thermophilic bacteria. The Journal of Agricultural Science **16**: 1-17.

85. Watnick, P., and Kolter, R. 2000. Biofilm, city of microbes. Journal of Bacteriology **182**(10): 2675-2679.

86. Weimer, P.J., Price, N.P.J., Kroukamp, O., Joubert, L.-., Wolfaardt, G.M., and Van Zyl, W.H. 2006. Studies of the extracellular glycocalyx of the anaerobic cellulolytic bacterium Ruminococcus albus 7. Applied and Environmental Microbiology **72**(12): 7559-7566.

87. Wiegel, J. 1981. Distinction between the gram reaction and the gram type of bacteria. International Journal of Systematic Bacteriology **31**(1): 88.

88. Wolfaardt, G.M., Lawrence, J.R., Robarts, R.D., Caldwell, S.J., and Caldwell, D.E. 1994. Multicellular Organization in a Degradative Biofilm Community. Appl. Environ. Microbiol. **60**(2): 434-446.

89. Wyman, C.E. 2008. Cellulosic ethanol: A unique sustainable liquid transportation fuel. MRS Bulletin **33**(4): 381-383.

90. Wyman, C.E., and Goodman, B.J. 1993. Biotechnology for production of fuels, chemicals, and materials from biomass. Applied Biochemistry and Biotechnology **39-40**(1): 41-59.

91. Yun, M.-., Yeon, K.-., Park, J.-., Lee, C.-., Chun, J., and Lim, D.J. 2006. Characterization of biofilm structure and its effect on membrane permeability in MBR for dye wastewater treatment. Water Research **40**(1): 45-52.

92. Zhang, Y., and Lynd, L.R. 2003. Quantification of cell and cellulase mass concentrations during anaerobic cellulose fermentation: Development of an enzyme-linked immunosorbent assay-based method with application to Clostridium thermocellum batch cultures. Analytical Chemistry **75**(2): 219-227.

93. Zhang, Y.-.P., and Lynd, L.R. 2005. Cellulose utilization by Clostridium thermocellum: Bioenergetics and hydrolysis product assimilation. Proceedings of the National Academy of Sciences of the United States of America **102**(20): 7321-7325.

94. Zhang, Y.-.P., and Lynd, L.R. 2004. Kinetics and Relative Importance of Phosphorolytic and Hydrolytic Cleavage of Cellodextrins and Cellobiose in Cell Extracts of Clostridium thermocellum. Applied and Environmental Microbiology **70**(3): 1563-1569.

APPENDICES

Appendix 1: Data for total non-attached cell counts and sample image of cell-counter software.

Table A1. 1. Upstream inoculation experiment: Cell count variation in duplicate samples and cell distribution per microscopic field

Time	Total cell counts (x10^5 cells/mL)	Std. Dev.	Percentage Std. Dev.	Average cells per field	Std. Dev.	Percentage Std. Dev.
26	19.45	-	-	69.4	13.59	19.58%
47	46.34	3.51	7.57%	165.3	31.15	18.84%
71	35.94	0.41	1.14%	115.4	16.37	14.19%
99	30.35	0.6	1.98%	97.45	12.82	13.16%
123	66.29	2.38	3.59%	23.38	4.87	20.83%

Table A1. 2. Downstream inoculation experiment: Cell count variation in duplicate samples and cell distribution per microscopic field

Time	Total cell counts (x10^5 cells/mL)	Std. Dev.	Percentage Std. Dev.	Average cells per field	Std. Dev.	Percentage Std. Dev.
24	20.37	1.55	7.61%	65.4	8.26	12.63%
47	8.17	0.23	2.82%	26.23	5.61	21.39%
70	10.13	0.53	5.23%	32.53	6.56	20.17%
95	11.84	1.42	11.99%	38.02	8.76	23.04%
124	23.52	0.47	2.00%	75.52	7.23	9.57%
145	30.26	0.95	3.14%	97.17	9.91	10.20%

Table A1. 3. Upstream inoculation experiment: Cell type percentage fraction

Time (h)	Percentage (%)		
	Normal Cells	Dividing cells (duplex)	Sporulated cells
0	0	0	0
26	68.7	28.01	3.29
47	84.83	13.03	2.14
71	85.62	9.99	4.39
99	81.88	10.4	7.72
123	81.83	8.8	9.97

Table A1. 4. Downstream inoculation experiment: Cell type percentage fraction.

Time (h)	Percentage (%)		
	Normal Cells	Dividing cells (duplex)	Sporulated cells
0	0	0	0
24	77.43	7.82	14.75
47	87.11	8.13	4.76
70	89.2	7.38	3.42
95	90.11	6.6	3.29
124	87.09	11.81	1.1
145	86.65	11.81	1.54

Sample calculations of total cell count – based on data in Table A1.5

The dimension of the Microscope Field = 225 µm x 280 µm and Field Area = 63000 μm^2 = 0.063mm^2

Total Area Counted = 30 fields x 0.063 mm^2 = 1.89 mm^2

Membrane Filtration Area = $\pi d^2/4$ = 176.625 mm^2 (where d = 15 mm)

Dilution = 10^{-1}; Volume sampled = 0.9 mL; Dilution factor (DF) = 1.11 (ml^{-1})

Total cells counted: Sample A = 3434; Sample B = 3490

Total cells in dilution = (Total cell counted*Membrane Area)/Total Area counted

Sample A = 320915.47; Sample B = 326148.80

Total cells in sample = Total cells in dilution x DF

Sample A = 35.65 x 10^5 cells/mL; Sample B = 36.23 x 10^5 cells/mL

Average = 35.94 x 10^5 cells/mL; Std. Dev = 0.41

Table A1. 5. Sample cell count (upstream inoculation – 71h of growth)

| Field	Total cells		Single cells		Dividing cells		Spore cells	
	Sample A	Sample B	Sample A	Sample B	Sample A	Sample B	Sample A	Sample B
1	104	124	91	106	6	8	1	2
2	105	94	84	79	6	5	9	5
3	119	158	109	130	3	9	4	10
4	113	133	99	103	4	12	6	6
5	136	90	117	75	7	6	5	3
6	119	91	105	78	5	4	4	5
7	136	95	117	78	7	7	5	3
8	128	115	111	99	6	5	5	6
9	114	124	101	99	3	8	7	9
10	101	114	79	98	9	7	4	2
11	107	150	93	126	5	9	4	6
12	103	99	90	84	4	6	5	3
13	102	141	85	121	6	8	5	4
14	110	116	93	99	5	6	7	5
15	135	135	119	122	6	3	4	7
16	133	125	117	110	3	5	10	5
17	114	93	92	76	7	6	8	5
18	110	104	97	87	4	6	5	5
19	125	82	109	73	6	3	4	3
20	100	85	84	76	5	3	6	3
21	114	85	101	71	4	5	5	4
22	104	111	91	99	4	4	5	4
23	126	117	109	98	7	6	3	7
24	107	143	91	118	6	7	4	11
25	106	132	94	113	5	6	2	7
26	119	139	108	123	4	6	3	4
27	102	150	91	129	4	7	3	7
28	110	122	93	104	6	7	5	4
29	110	113	93	94	5	7	7	5
30	122	110	109	88	5	8	3	6
TOTAL	3434	3490	2972	2956	157	189	148	156
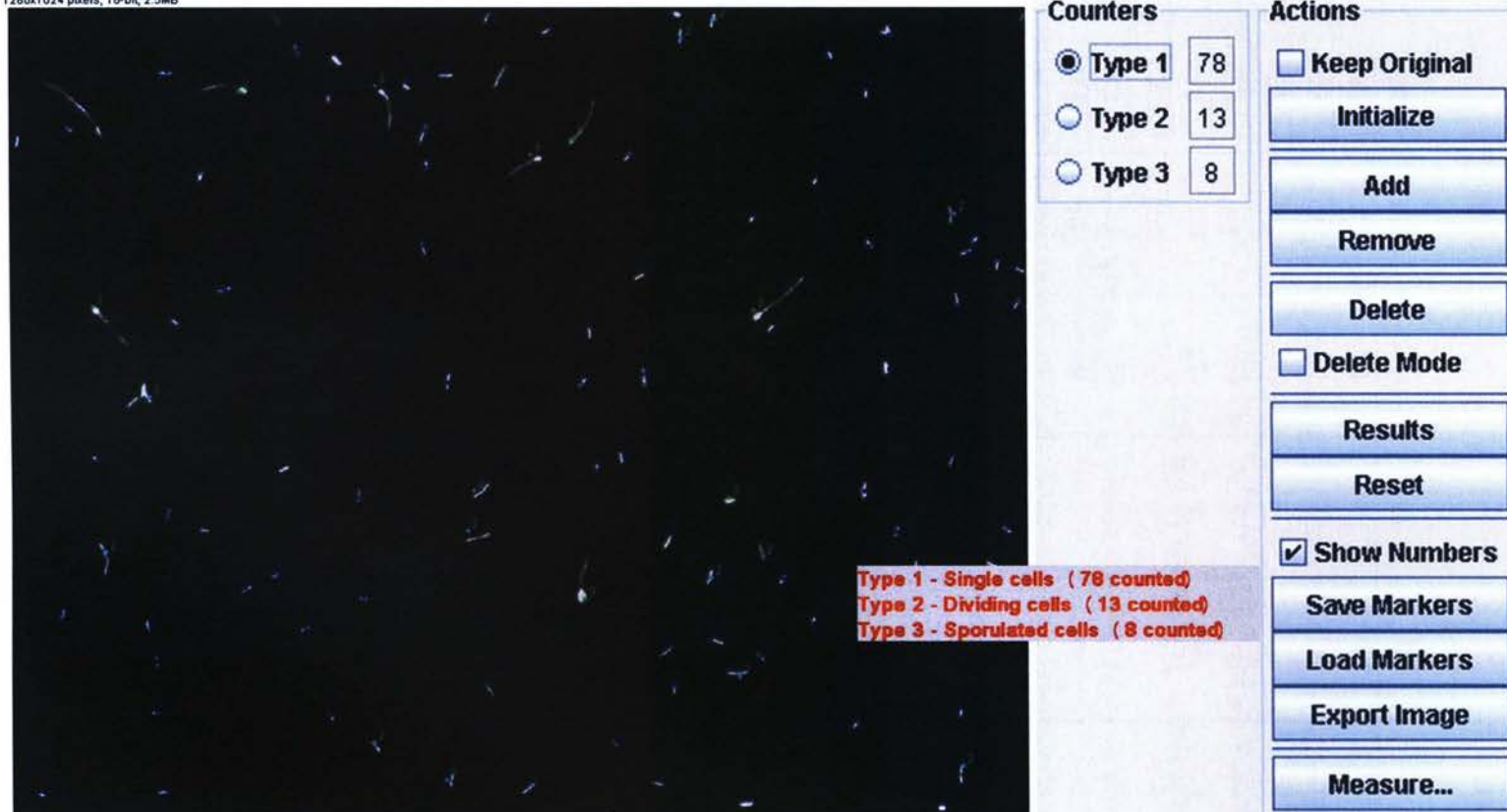
Figure A. 1 Sample image of ImageJ cell counter tool
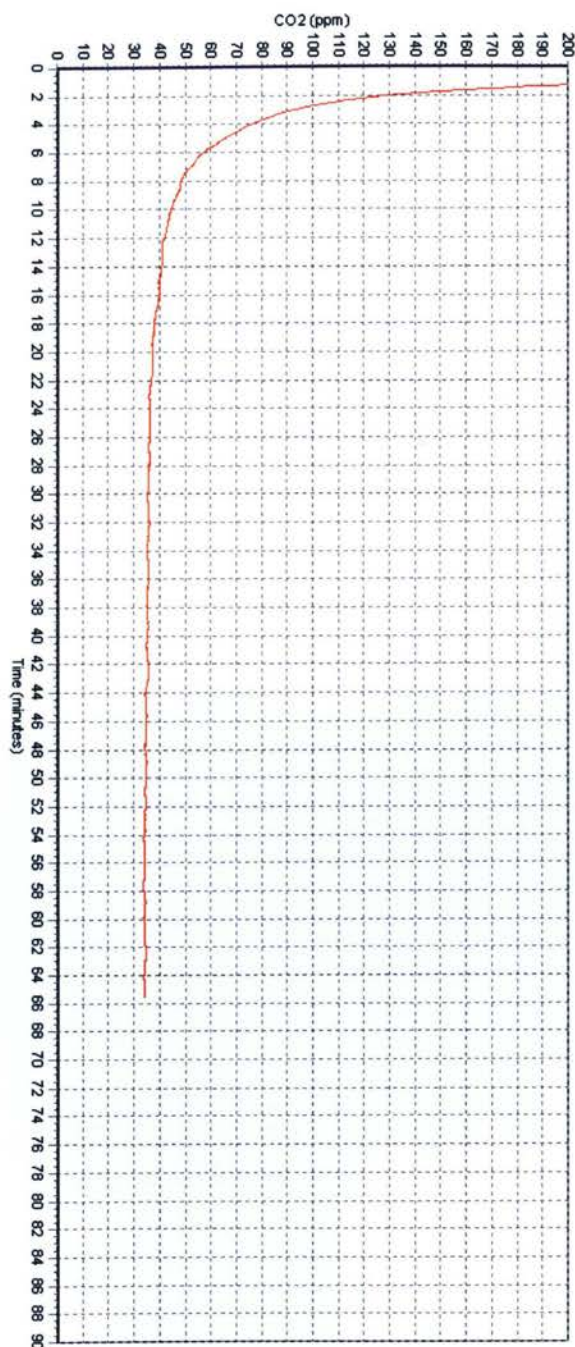
Appendix 2: Carbon Dioxide Sample Data Monitor

Figure A. 2 Gaseous carbon dioxide measurements in biofilm effluent after 72 hours of growth (value stabilizes at 34.2 ±0.1 ppm)

Appendix 3: Data for total carbohydrate concentration in effluent samples

Table A3.1 Upstream inoculation experiment: Total Carbohydrate in effluent samples

Glucose std*.	H2O	5% Phenol	conc. H2SO4	Final Volume
(μL)	(μL)	(μL)	(mL)	(μL)
0	500	500	2	3000
50	450	500	2	3000
100	400	500	2	3000
150	350	500	2	3000
200	300	500	2	3000

STANDARD CURVE

[Glucose]		Absorbance	
(μg/mL)	STD A	STD B	STD (average)
Blank	0	0	0
3.33	0.1025	0.1016	0.1021
6.67	0.1966	0.2254	0.2110
10.00	0.3102	0.2975	0.3039
13.33	0.4143	0.3957	0.4050

Samples

Time		Absorbance		
(hours)	Sample 1	Sample 2	Sample 3	Sample (average)
0	0.1780	0.1510	0.1602	0.1631
26	0.1386	0.1396	0.1509	0.1430
47	0.1587	0.1635	0.1830	0.1684
71	0.1746	0.1653	0.1797	0.1732
99	0.1591	0.1505	0.1547	0.1548
123	0.1327	0.1448	0.1504	0.1426

[CONCETRATION] DILUTION ADJUSTED** (μg/mL)

Sample 1	Sample 2	Sample 3	Sample (average)	Variance	Std. Dev.
115.33	97.33	103.47	105.38	83.74	9.15
89.07	89.73	97.27	92.02	20.74	4.55
102.47	105.67	118.67	108.93	73.61	8.58
113.07	106.87	116.47	112.13	23.69	4.87
102.73	97.00	99.80	99.84	8.22	2.87
85.13	93.20	96.93	91.76	36.37	6.03

* Glucose standard used: 200μg/mL (prepared in 0.002g/L Resazurin solution)

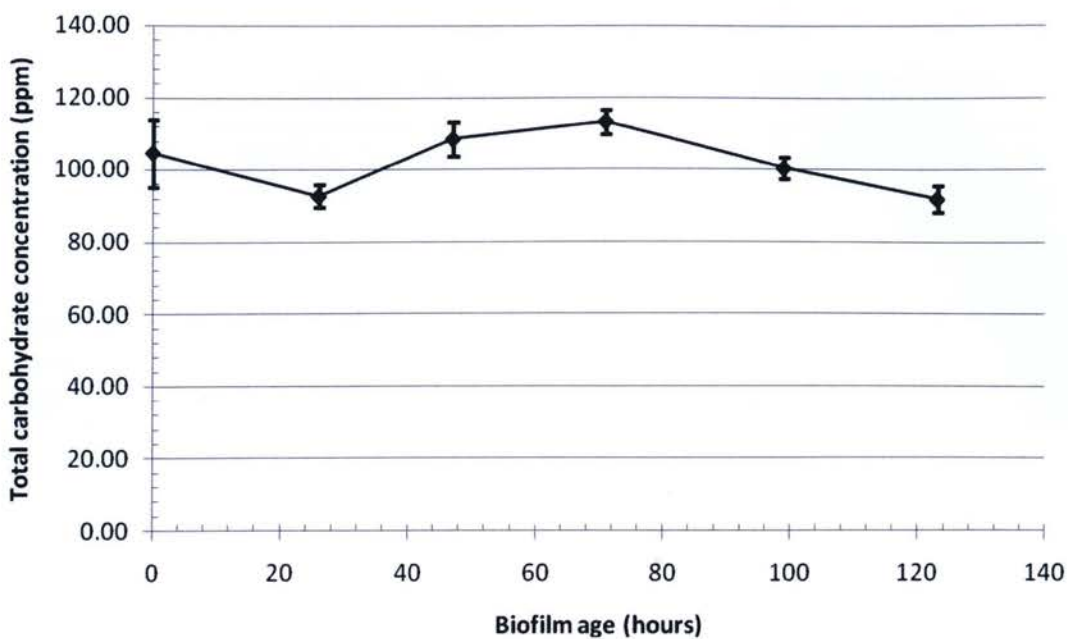** Sample volume used in the reaction mix = 150μl   => Dilution factor = 3000/150 = 20

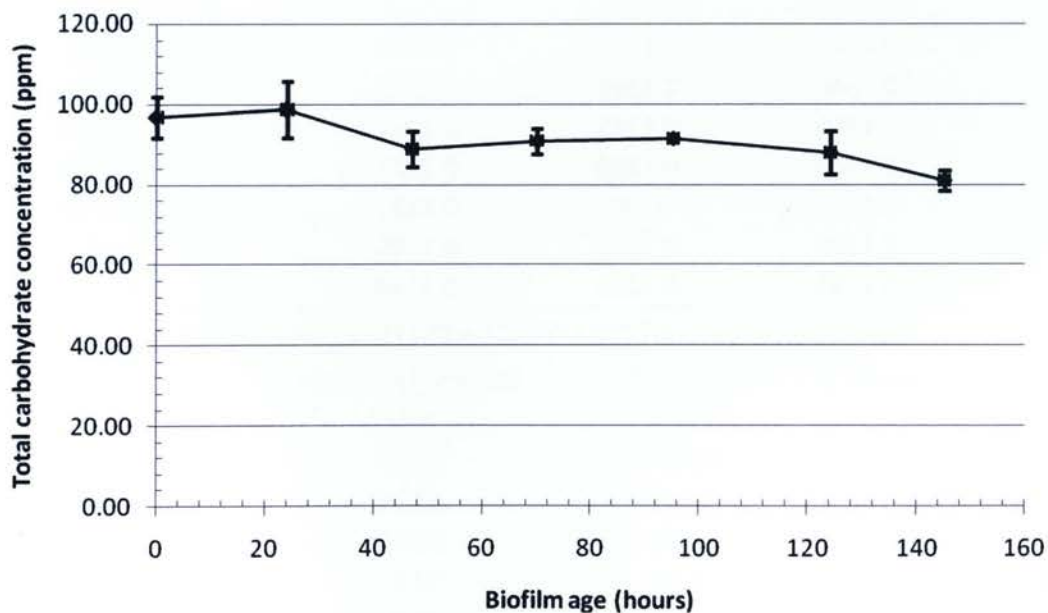Figure A. 3 Upstream inoculation experiment: Total Carbohydrate variation in effluent sampling

Figure A. 4 Downstream inoculation experiment: Total Carbohydrate variation in effluent sampling

93

Table A3.2. Downstream inoculation experiment: Total Carbohydrate in effluent samples

Glucose std*. (µL)	H2O (µL)	5% Phenol (µL)	conc. H2SO4 (mL)	Final Volume (µL)
0	500	500	2	3000
50	450	500	2	3000
100	400	500	2	3000
150	350	500	2	3000
200	300	500	2	3000

STANDARD CURVE

[Glucose] (µg/mL)	Absorbance		
	STD A	STD B	STD (average)
Blank	0	0	0
3.33	0.0816	0.1006	0.0911
6.67	0.1824	0.1949	0.1887
10.00	0.2850	0.2658	0.2754
13.33	0.3441	0.3974	0.3708

Samples

Time (hours)	Absorbance			
	Sample 1	Sample 2	Sample 3	Sample (average)
0	0.1344	0.1386	0.1485	0.1405
24	0.1546	0.1399	0.1348	0.1431
47	0.1356	0.1285	0.1227	0.1289
70	0.1286	0.1298	0.1371	0.1318
95	0.1328	0.132	0.1331	0.1326
124	0.1283	0.1349	0.1195	0.1276
145	0.1135	0.1202	0.1184	0.1174

[CONCETRATION] DILUTION ADJUSTED** (µg/mL)

Sample 1	Sample 2	Sample 3	Sample (average)	Variance	Std. Dev.
92.69	95.59	102.41	96.90	24.93	4.99
106.62	96.48	92.97	98.69	50.27	7.09
93.52	88.62	84.62	88.92	19.85	4.46
88.69	89.52	94.55	90.92	10.07	3.17
91.59	91.03	91.79	91.47	0.15	0.39
88.48	93.03	82.41	87.98	28.39	5.33
78.28	82.90	81.66	80.94	5.72	2.39

* Glucose standard used: 200µg/mL (prepared in 0.002g/L Resazurin solution)
** Sample volume used in the reaction mix = 150µl   => Dilution factor = 3000/150 = 20